Please cite this article in press as: Natu et al., A critical analysis of the X-ray photoelectron spectra of $Ti_3C_2T_z$ MXenes, Matter (2021), https://doi.org/10.1016/j.matt.2021.01.015

Matter

CellPress

Review

A critical analysis of the X-ray photoelectron spectra of $Ti_3C_2T_z$ MXenes

Varun Natu,[1] Mohamed Benchakar,[2] Christine Canaff,[2] Aurélien Habrioux,[2] Stéphane Célérier,[2] and Michel W. Barsoum[1,*]

SUMMARY

Since their discovery in 2011, MXenes have garnered worldwide interest. Given their 2D structure, surface, or termination, chemistries play a vital role in most applications. X-ray photoelectron spectroscopy (XPS) is one of the most common characterization tools for quantifying surface terminations and overall chemistry. Herein, we critically review the XPS fitting models proposed for $Ti_3C_2T_z$ MXene in the literature and make the case that they are at best incomplete and at worst contradictory. We propose a new fitting algorithm based on all the data obtained from previously published studies and propose a new method for quantifying the surface terminations in $Ti_3C_2T_z$. In our approach, we assign the Ti 2p peak at 455.1 eV to the C–Ti–O\O\O, and the peaks at 456.0, 457.0, 457.9, and 459.6 eV are assigned to C–Ti–O\O\F, C–Ti–O\F\F, C–Ti–F\F\F, and $TiO_{2-x}F_{2x}$, respectively. The first four represent possible Ti atom terminations; the last is an oxyfluoride. The C 1s peak at 282 eV, ascribed to C atoms surrounded by 6 Ti atoms, is so universal that it can almost be used as a reference.

INTRODUCTION

After the discovery of 2D titanium carbide ($Ti_3C_2T_z$), the first MXene, in 2011, nearly 30 new MXenes have been discovered in the last decade, and several others are predicted to be stable according to computational calculations and are awaiting experimental realization.[1,2] MXenes show potential in various applications like energy storage and conversion,[3,4] photodetectors and sensors,[5] catalysts for various reactions,[6] reinforcement in polymer composites,[7] and electromagnetic interference (EMI) shielding,[8] among many others. MXenes are so labeled because they are obtained by selective etching of the A atomic layers from the parent MAX phases. The MAX phases have a general formula of $M_{n+1}AX_n$ where M stands for an early transition metal, X stands for C and/or N, and A is mostly a group 13 or 14 element.[9–11] When the A layers, mostly Al, are etched, they are replaced by surface terminations, so the general formula of MXenes is $M_{n+1}X_nT_z$, where T_z represents surface terminations that are typically a combination of –O, –OH, and/or –F.[12] The -ene suffix was added to signify their similarity to other 2D materials like graphene.[1] The recently discovered MXene synthesis technique of using molten salt to etch out the A layer leads to terminations like –Cl, –Br, and –I, and further chemical modifications can also result in –S, –Te, and –NH terminations.[13,14]

Given the 2D morphology of MXenes, their surface chemistries play an important role in determining their properties. For example, surface terminations are responsible for the spontaneous ion intercalation and exchange in between MXene

Progress and potential

Interest in MXenes is quite high because of their potential in a wide range of applications. Although several MXenes have been discovered to date, most studies so far have focused mainly on $Ti_3C_2T_z$. Given their 2D nature and rich surface chemistry, XPS is the preferred technique for analyzing their compositions. To date, only four studies have focused on understanding and fitting the XPS spectra on $Ti_3C_2T_x$ flakes. While there are commonalities between the various fitting protocols, there are also some inconsistencies that have sown confusion. In this review, we summarize the XPS fitting models proposed especially for $Ti_3C_2T_z$ and propose a new fitting model based on critical analysis of previously published studies. We also point out areas where more work is needed to better understand the XPS spectra. We feel this article will help researchers to better analyze their data using XPS for MXenes and other 2D materials.

Please cite this article in press as: Natu et al., A critical analysis of the X-ray photoelectron spectra of $Ti_3C_2T_z$ MXenes, Matter (2021), https://doi.org/10.1016/j.matt.2021.01.015

layers.[15] They are also responsible for the hydrophilicity of MXenes, which renders them one of the most easily processable 2D materials.[16] In energy storage devices like supercapacitor and batteries, MXene surface terminations are shown to participate in the charge storage mechanism.[3] Recent work by Kamysbayev et al.[14] showed that superconductivity in Nb_2CT_z is dependent on the type of surface terminations. The work function of MXenes can also be tuned by modifying its surface groups, making them good electronic contacts in circuits.[17] Apart from these applications, MXene surface terminations have also been shown to play a role in influencing optical, mechanical, magnetic, and a multitude of other properties.[18]

Due to the critical role surface terminations play on properties, it is important to characterize them properly. There a number of techniques that can do so, including X-ray photoelectron spectroscopy (XPS), X-ray adsorption spectroscopy (XAS),[19] NMR spectroscopy,[20,21] Raman spectroscopy,[22] and transmission electron microscopy (TEM) coupled with electron energy loss spectroscopy (EELS).[23,24] XPS remains the most widely used of all the techniques. There are several advantages of using XPS to analyze MXenes, as it is sensitive to all light elements except H and He.[25] It can be used to analyze bonding environments of constituent elements, quantify elemental compositions, including terminations, and detect small concentrations of elements, especially if they are at the surfaces.[25] Other advantages include non-destructive sample preparation and the fact that restrictions on sample size and form are low. XPS spectrometers are widely available in most university settings and large research and development laboratories.

To date, four studies have focused on understanding and fitting XPS spectra on $Ti_3C_2T_z$ flakes.[12,17,26,27] And while there are similarities between the various fitting protocols, there are also some inconsistencies that can sow confusion in interpreting results. In this review, we summarize these fitting models for $Ti_3C_2T_z$, and propose a new fitting model, based on the critical analysis of previously published studies. In our model, we fit the XPS spectra based on the nature of the surface termination surrounding each Ti atoms, rather than their oxidation states as many, including us, have previously done. We also argue that the ambiguity in fitting the peaks is higher in the O and F spectra as compared with those of Ti and C.

Before going into a detailed discussion of the various fits, it should be noted that the Ti 2p spectrum has two peaks at roughly 455 and 463 eV, corresponding to Ti $2p_{3/2}$ and Ti $2p_{1/2}$, respectively. The split is due to spin-orbit splitting, and both peaks contain information about the Ti bonding environment. Therefore, when component peak fitting is used to deconvolute these peaks, all components that fit under the Ti $2p_{3/2}$ peak also fit in the Ti $2p_{1/2}$ peak (further details are given later). Component peaks are fitted to understand what species of Ti are present and from here onwards in the discussion of the various regions whenever peaks are mentioned we refer to the component peaks used to fit the spectra and not the envelope peaks. In the following sections, we review the various fits.

Fit-I

The first detailed study dedicated to understanding the XPS spectra of $Ti_3C_2T_z$ was carried out by Halim et al.[12] in 2016. They based their fittings on the oxidation states of Ti and attribute the first three peaks at 455.0 eV, 455.8 eV, and 457.2 eV to Ti^{+1}, Ti^{+2}, Ti^{+3} oxidation states, respectively (Figure 1A, Table 1). The peak separation between the Ti $2p_{3/2}$ and $2p_{1/2}$, Δ_{Ti2p}, caused by spin-orbit splitting (see below) was kept fixed at 6.2 eV, 5.5 eV, and 5.7 eV for the Ti^{+1}, Ti^{+2}, Ti^{+3} peaks, respectively (Table 1).[12] This Δ_{Ti2p} is consistent with other XPS studies on Ti metal and related

[1]Department of Materials Science and Engineering, Drexel University, Philadelphia, PA 19104, USA

[2]Institut de Chimie des Milieux et Matériaux de Poitiers (IC2MP), Université de Poitiers, CNRS, 86073 Poitiers, France

*Correspondence: barsoumw@drexel.edu

https://doi.org/10.1016/j.matt.2021.01.015

Please cite this article in press as: Natu et al., A critical analysis of the X-ray photoelectron spectra of $Ti_3C_2T_z$ MXenes, Matter (2021), https://doi.org/10.1016/j.matt.2021.01.015

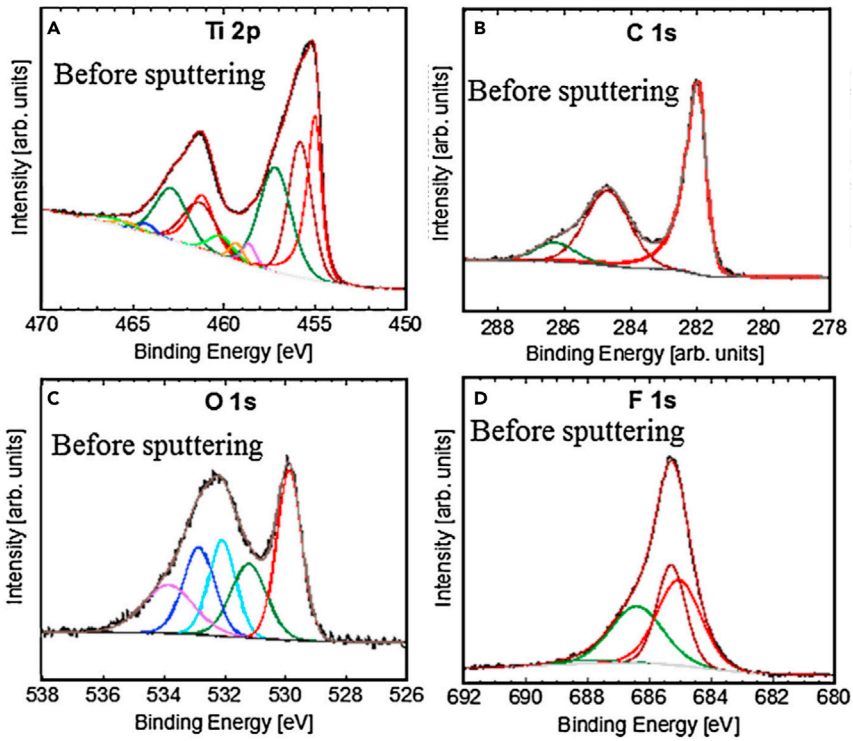

Figure 1. Component peak fits of XPS spectra of as-prepared $Ti_3C_2T_z$ powders
High-resolution component peak fits of (A) Ti 2p, (B) C 1s, (C) O 1s, and (D) F 1s regions.[12] Reprinted from Halim et al.,[12] copyright (2021), with permission from Elsevier.

compounds such as titanium carbide, TiC, where the peak separation is found to be ~6.1–6.2 eV. The Δ_{Ti2p} in TiO (Ti^{+2}) is ~5.6–5.7 eV and that for Ti_2O_3 (Ti^{+3}) is ~5.7 eV.[28,29] In our proposed fit (see below), a Δ_{Ti2p} of 6.1 eV was used for all Ti peaks related to $Ti_3C_2T_z$.

The C–Ti–F component peak was set at 460.2 eV, with a Δ_{Ti2p} of 6 eV (Table 1). These values are consistent with fluorinated Ti compounds like TiF_3.[30] The last set of Ti peaks found around 459.3 eV (Δ_{Ti2p} = 5.6 eV) and 460.2 eV (Δ_{Ti2p} = 6 eV) (Figure 1A, Table 1) were ascribed to TiO_2 and $TiO_{2-x}F_{2x}$ oxides, respectively, formed due to the degradation/oxidation of $Ti_3C_2T_z$ by reaction with ambient air and/or water. Note that Halim et al.[12] assumed these two components not to originate from the $Ti_3C_2T_z$ flakes themselves, but rather from their oxides and oxyfluorides. We make the same assumption below.

Irrespective of the type of termination present, the C 1s high-resolution spectra associated with $Ti_3C_2T_z$ all appear in the quite narrow range of ≈281.9–282.0 eV (Figure 1B, Table 1). This signal originates from C atoms residing in the Ti octahedra. The rest of the components are typically ascribed to C contamination introduced during synthesis or from ambient air. This is so universal in $Ti_3C_2T_z$ synthesized in F-ion-containing acids that it can be used as a check on the calibration of the XPS spectra. As discussed below, there are some exceptions..

In the O 1s spectra (Figure 1C, Table 1), two components associated with $Ti_3C_2T_z$ flakes were set at 531.2 eV and 532.0 eV and ascribed to –O and –OH terminations, respectively. Three other peaks were added to the fitting at 529.9 eV, 532.8 eV, and

Please cite this article in press as: Natu et al., A critical analysis of the X-ray photoelectron spectra of $Ti_3C_2T_z$ MXenes, Matter (2021), https://doi.org/10.1016/j.matt.2021.01.015

Table 1. Summary of XPS peak fits

Region	BE (eV)	FWHM (eV)	Fraction	Assigned to
Ti $2p_{3/2}$ ($2p_{1/2}$)	455.0 (461.2)	0.8 (1.5)	0.28	C–Ti–(O/OH)
	455.8 (461.3)	1.5 (2.2)	0.30	C–Ti^{2+}–(O/OH)
	457.2 (462.9)	2.1 (2.1)	0.32	C–Ti^{3+}–(O/OH)
	458.6 (464.2)	0.9 (1.0)	0.02	TiO_2
	459.3 (465.3)	0.9 (1.4)	0.03	$TiO_{2-x}F_{2x}$
	460.2 (466.2)	1.6 (2.7)	0.05	C–Ti–F
C 1s	282.0	0.6	0.54	C–Ti–(O/OH/F)
	284.7	1.6	0.38	C–C
	286.3	1.4	0.08	CH_x/C–O
O 1s	529.9	1.0	0.29	TiO_2
	531.2	1.4	0.18	C–Ti–O_x and/or OR
	532.0	1.1	0.18	C–Ti–OH_x and/or OR
	532.8	1.2	0.19	Al_2O_3 and/or OR
	533.8	2.0	0.17	H_2O and/or OR
F 1s	685.0	1.7	0.38	C–Ti–F
	685.3	1.1	0.29	$TiO_{2-x}F_{2x}$
	686.4	2.0	0.30	AlF_x
	688.3	2.0	0.02	$Al(OF)_x$

The $Ti_3C_2T_z$ sample was prepared by etching the MAX phase in 48% HF. BE and FWHM values of the Ti $2p_{3/2}$ peaks are listed in columns 2 and 3, respectively. Respective numbers for Ti $2p_{1/2}$ peaks are shown in brackets. These peak fits are given by Halim et al.,[12] shown in Figure 1.

533.8 eV corresponding to, respectively, TiO_2, Al_2O_3, and adsorbed or interlayer water, respectively (Table 1). Contributions from C–O, C=O, –COOH, etc. species from the adventitious C tend to overlap with the components described earlier, making their estimation difficult and probably leading to overestimation of some of the components in the O 1s spectra.

The F 1s spectra were fitted with four components corresponding to C–Ti–F, $TiO_{2-x}F_{2x}$, AlF_x, and $Al(OF)_x$ at 685.0, 685.3, 686.4, and 688.3 eV, respectively. With only 38% of the total photoemission spectra attributed to the C–Ti–F of the MXene itself, the majority was due to the aforementioned impurities.

Henceforth, this model proposed by Halim et al.[12] will be referred to as Fit-I.

Fit-II

Persson et al.[26] proposed a different fitting model. They based their fits on the crystal sites that the various atoms occupy.[26] When dealing with the Ti spectra, they differentiated between C–Ti–O\O\O, C–Ti–(O,F), and C–Ti–F\F\F. In this notation, used henceforth, the atoms separated by "\" are the terminations present. For example, C–Ti–O\O\O corresponds to Ti atoms in octahedra with 3 C atoms and 3 O surface atoms at the vertices. In C–Ti–F\F\F, all the terminations are F. The notation C–Ti–(O,F) represents mixed O and F terminations.[26]

Their fits are based on density functional theory (DFT) calculations by Khazaei et al.[31] who found two thermodynamically favorable sites on MXene surfaces: A sites corresponding to surface groups occupying positions above the central Ti atom (so-called FCC sites) and B sites corresponding to surface groups above the C atoms right below the surface Ti atoms (Figures 2D and 2E).

The Ti $2p_{3/2}$ peak was fitted with three components corresponding to C–Ti–O\O\O, C–Ti–(O,F), and C–Ti–F\F\F at 455.1 eV, 455.9 eV, and 456.9 eV, respectively (Figure 2C,

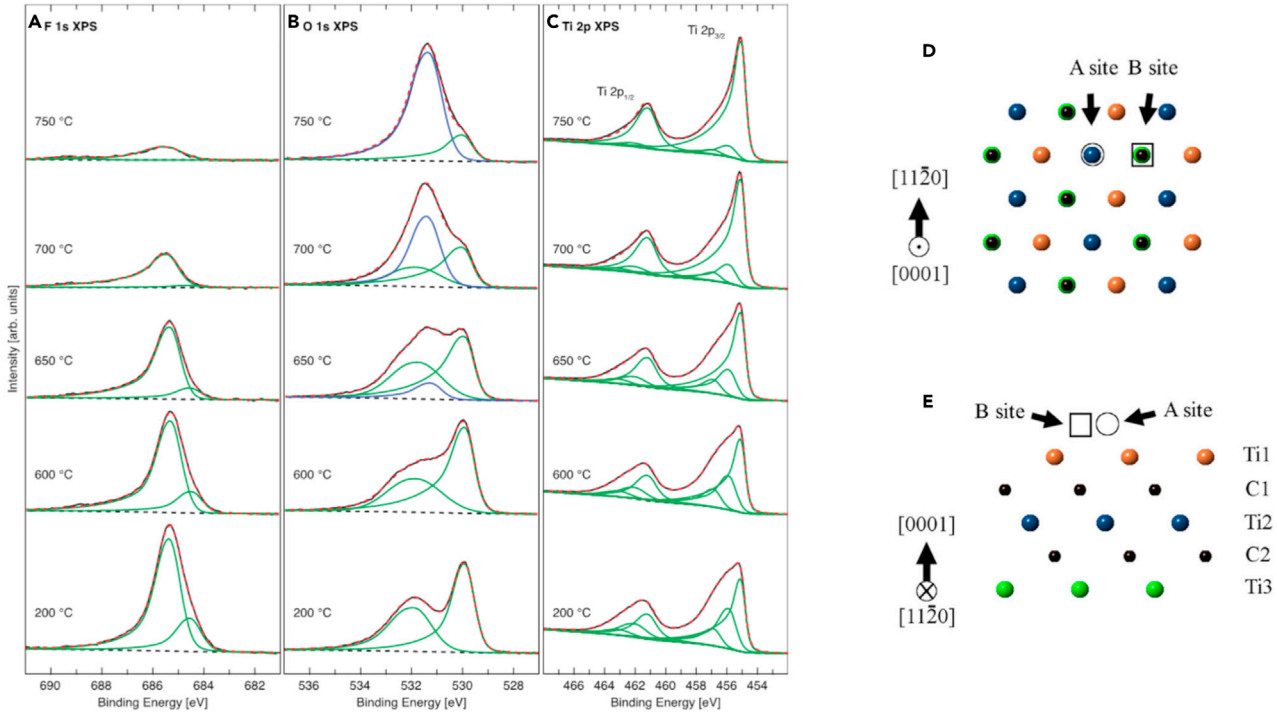

Figure 2. Peak fits of XPS spectra of $Ti_3C_2T_z$ MXene during *in situ* vacuum annealing inside an XPS chamber at various temperatures

High-resolution component peak fits of, (A) F 1s, (B) O 1s, (C) Ti 2p, and (D) F1s regions; (D) top and (E) side view with A and B possible termination sites.[26] This image is licensed under CC BY-ND 2.0 (https://creativecommons.org/licenses/by-nd/2.0/).

Table 2). As just noted, because Persson et al.[26] do not distinguish between the C–Ti–O\O\F, C–Ti–O\F\F configurations, they only assigned one peak for the two at 455.9 eV. The Δ_{Ti2p} was kept constant for all components and fixed at 6.1 eV. Also, no oxide peaks were included in the fits as the authors scanned MXenes right after etching and washing with minimal exposure to ambient air.

The O 1s spectra were fitted with three peaks, two of which were assigned to –O terminations occupying the A and bridging sites, while the third was assigned to an –O co-

Table 2. Summary of XPS peak fits

Region	BE (eV)	FWHM (eV)	Assigned to
Ti $2p_{3/2}$ ($2p_{1/2}$)	455.1 (461.2)	0.7 (1.4)	C–Ti–O\O\O
	455.9 (462.0)	1.1 (1.9)	C–Ti–(O, F)
	456.9 (463.0)	1.1 (1.9)	C–Ti–F\F\F
C 1s	282.0	0.64	Ti–C–Ti
	284.3	1.3	C–C
	285.2	1.3	CH_x
	286.4	1.3	C–OH
O 1s	529.9	0.89	C–Ti–O (bridging)
	531.3	1.2	C–Ti–O (A site)
	531.9	1.6–2.3	C–Ti–O/F (A site)
F 1s	684.5	1.0	C–Ti–F
	685.4	1.0	C–Ti–O, F

The $Ti_3C_2T_z$ sample was prepared by etching the MAX phase in 10% HF. BE and FWHM values of Ti $2p_{3/2}$ peaks are listed in columns 2 and 3, respectively. Respective numbers for the Ti $2p_{1/2}$ peaks are shown in brackets.[26] This summary is only of the fits after annealing at 200°C. These are the peaks fits shown in Figure 2.

Please cite this article in press as: Natu et al., A critical analysis of the X-ray photoelectron spectra of $Ti_3C_2T_z$ MXenes, Matter (2021), https://doi.org/10.1016/j.matt.2021.01.015

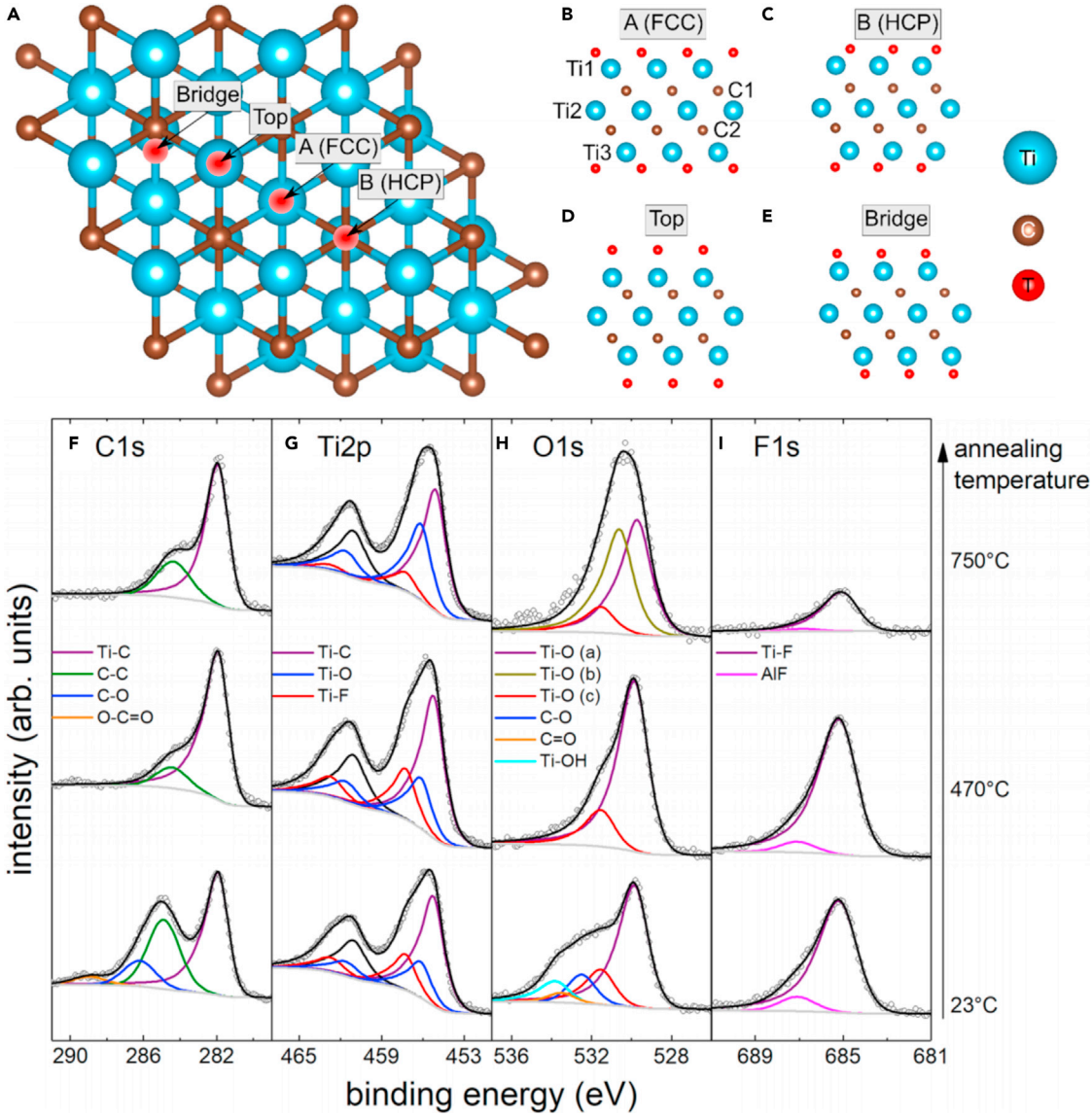

Figure 3. Peak fits of XPS spectra of $Ti_3C_2T_z$ during *in situ* vacuum annealing inside an XPS chamber at various temperatures

(A) Top and (B–E) side views with possible termination sites. Peak fits of XPS spectra of $Ti_3C_2T_z$ during *in situ* vacuum annealing inside an XPS chamber at various temperatures. High-resolution component peak fittings of, (F) C 1s, (G) Ti 2p, (H) O 1s, and (I) F1s region.[17] Reprinted (adapted) with permission from Ref.[17]. Copyright (2021) American Chemical Society.

absorbed with –F on the A sites. The respective energies were 531.3, 529.9, and 531.9 eV (Figure 2B, Table 2). Similarly, in the F 1s spectra, two peaks were observed at 684.5 eV and 685.4 eV corresponding to –F terminations and –F terminations co-adsorbed with O (Figure 2A, Table 2). Similar to Fit-I, only one C 1s peak at 282.0 eV was ascribed to the MXene flakes; the rest were ascribed to adventitious C contaminations.

This fitting model will henceforth be referred to as Fit-II.

Fit-III

Similar to Persson et al.[26], Schultz et al.[17] also measured XPS *in situ* as a function of heating but they used a different fitting model (Figure 3, Table 3). Three components were fit to the Ti $2p_{3/2}$ spectra (Figure 3G) corresponding to C–Ti–C, C–Ti–O,

Please cite this article in press as: Natu et al., A critical analysis of the X-ray photoelectron spectra of $Ti_3C_2T_z$ MXenes, Matter (2021), https://doi.org/10.1016/j.matt.2021.01.015

Table 3. Summary of XPS peak fits

Region	BE (eV)	Assigned to
Ti $2p_{3/2}$ ($2p_{1/2}$)	455.2 (461.1)	Ti–C
	456.2 (461.6)	Ti–O
	457.3 (462.7)	Ti–F
C 1s	281.9	Ti–C–Ti
	284.9	C–C
	286.2	C–O
	288.9	C=O
O 1s	529.8	C–Ti–O (bridge)
	531.6	C–Ti–O (A/B site)
	532.5	C–O
	533.4	C=O
	533.8	adsorbed H_2O or C–Ti–OH
F 1s	685.2	C–Ti–F
	687.1	F contamination

Sample was prepared by etching Ti_3AlC_2 in a LiF + HCl mixture. Numbers in brackets in column 2 are peak locations for Ti $2p_{1/2}$, while the BE values for the Ti $2p_{3/2}$ peaks are listed outside the brackets.[17] These values correspond to fits of spectra collected at RT. These are the peaks fits shown in Figure 3.

and C–Ti–F at 455.2 (Δ_{Ti2p} = 5.9 eV), 456.2 (Δ_{Ti2p} = 5.4 eV) and 457.3, eV (Δ_{Ti2p} = 5.4 eV), respectively (Figure 3G, Table 3). The first peak was assigned to Ti bonded to C only (i.e., the central Ti atoms labeled Ti2 in Figure 3B), while the second and third peaks were assigned to Ti atoms bonded to pure O and pure F terminations, respectively (Figure 3G). In this model, the assumption was made that the central Ti atoms surrounded octahedrally with 6 C atoms can be differentiated from the ones closer to the surfaces. As discussed below, such differentiation is not trivial, to say the least.

In the O 1s spectra, three related components were fitted at 529.8, 531.6, and 533.8 eV, corresponding to bridging O terminations (Figure 3H), O terminations at A/B sites (Figures 3B and 3C), and OH terminations at A/B sites. Schultz et al.[17] claimed that the OH component overlaps with adsorbed water, making those two difficult to distinguish. Only one component for the C and F spectra corresponding to MXene was fitted at 281.9 eV and 685.2 eV, respectively, the remainder were ascribed to impurities (Figures 3F and 3I, Table 3). Henceforth this fit will be referred to as Fit-III. The substantial differences between this fit and the previous two should be clear at this point.

Fit-IV

In a recent paper, Benchakar et al.[27] used a similar approach to that of Halim et al.[12] in the Ti 2p region, except the component at ~ 460.0 eV, which was ascribed to –F terminations by Halim et al.,[12] was ascribed to a titanium fluoride (TiF_x) salt formed due to over-etching (Figure 4, Table 4).[27]

The O 1s fits, on the other hand, used aspects of Fit-I and Fit-III. The –O terminations at the A and the bridging sites were similar to those of Fit-III (Tables 1, 3, and 4), respectively assigned to C–Ti–O(ii) and C–Ti–O(i) in Table 4 and Figure 4. An –OH component similar to Fit-I was also assumed. Peaks for organic contamination and $TiOF_2$ ($TiO_{2-x}F_{2x}$) were also added. Note that the contribution of TiO_2 and $TiOF_2$ in the O1s region at 530.6 and 529.9 eV, respectively, are not the same as those of Halim et al.[12] Similar to previous studies, only one component in the F 1s and C 1s regions was fitted (Figure 4, Table 4). Henceforth, this model will be referred to as Fit-IV.

Please cite this article in press as: Natu et al., A critical analysis of the X-ray photoelectron spectra of $Ti_3C_2T_z$ MXenes, Matter (2021), https://doi.org/10.1016/j.matt.2021.01.015

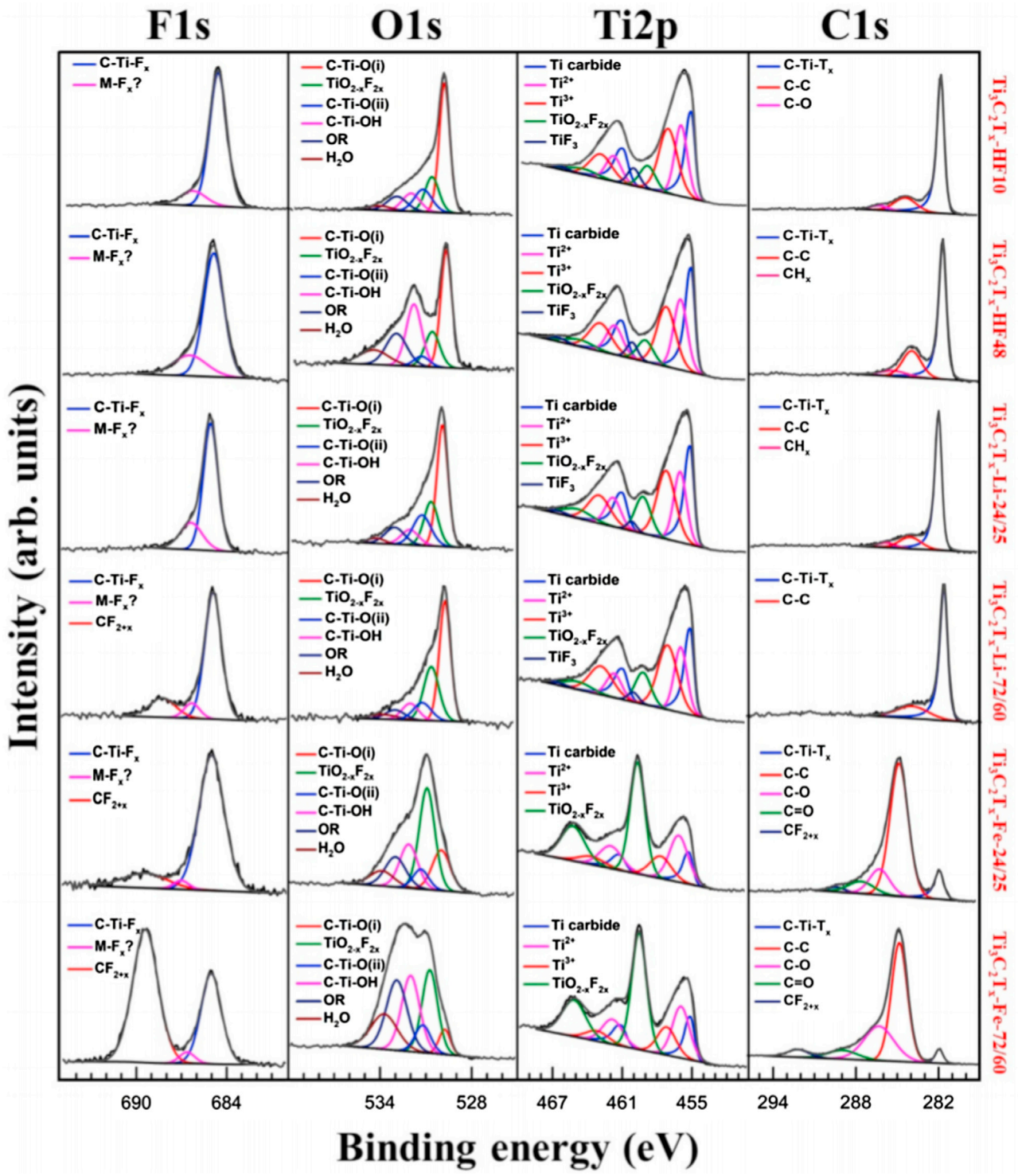

Figure 4. Peak fits of XPS spectra of $Ti_3C_2T_z$ synthesized using different conditions indicated on the right-hand side.

In Table 4, we only list the results of the topmost panels, *viz.* MXene etched using 10% HF. Reprinted from Benchakar et al.,[27] copyright (2021), with permission from Elsevier.

Please cite this article in press as: Natu et al., A critical analysis of the X-ray photoelectron spectra of $Ti_3C_2T_z$ MXenes, Matter (2021), https://doi.org/10.1016/j.matt.2021.01.015

Table 4. Summary of XPS peak fits for MXene synthesized using 10% HF

Region	BE (eV)	FWHM (eV)	Fraction	Assigned to
Ti $2p_{3/2}$ ($2p_{1/2}$)	455.0(461.0)	0.8 (1.1)	9.95	C–Ti^{+1}–(O/OH/F)
	455.8 (461.7)	1.3 (1.6)	10.16	C–Ti^{2+}–(O/OH/F)
	457.0 (462.8)	1.9 (2.3)	12.54	C–Ti^{3+}–(O/OH/F)
	458.9 (464.6)	1.6 (2.9)	3.76	$TiO_{2-x}F_{2x}/TiO_2$
	460.0 (466.4)	1.2 (1.8)	1.87	TiF_x
C 1s	281.9	0.6	22.65	C–Ti–(O/OH/F)
	284.4	1.8	5.22	C–C
	286.4	1.9	0.74	C–O
O 1s	529.7	0.8	8.86	C–Ti–O(i)
	530.6	1.2	3.15	$TiO_{2-x}F_{2x}$
	531.2	1.4	2.55	C–Ti–O(ii)
	532.0	1.4	2.04	C–Ti–OH
	533.0	1.5	1.85	OR
	533.7	2.2	0.69	H_2O
F 1s	685.0	1.3	12.30	C–Ti–F
	686.6	1.6	1.65	F contamination

BE and FWHM values of the Ti $2p_{3/2}$ peaks are listed in columns 2 and 3, respectively. Respective numbers for Ti $2p_{1/2}$ peaks are shown in brackets.[27] These are the peaks fits shown in Figure 4.

Critical analysis

Based on these four studies, it is clear that there is no clear consensus in the MXene community about the interpretation of $Ti_3C_2T_z$ XPS spectra. In Fit-I, Fit-II, and Fit-IV, the first peak in the Ti $2p_{3/2}$ spectra is at ~455.0 eV and is assigned to C–Ti–T_z, while in Fit-III it is assigned to Ti–C–Ti. The discrepancies in binding energies (BEs) of the C–Ti–F components are even larger than those of C–Ti–O. In Fit-I and Fit-II there is a 3.3 eV difference in the BEs of the respective C–Ti–F peaks. In Fit-I and Fit-III, that difference is 2.9 eV. Fit-IV does not account for a separate C–Ti–F peak since it is claimed that these peaks overlap with those of the C–Ti–O/OH peaks and thus cannot be distinguished. Apart from these two peaks, other peaks in Fit-I, Fit-II, and Fit-III are assigned to different species, making a direct comparison between the BEs impossible. Needless to add, these are serious problems. What renders the problem even more confusing is that most other studies that use XPS for characterization of $Ti_3C_2T_z$ use either of these four models or, in some cases, even a mix of them. The purpose of this paper is to critically assess these four fits and recommend a less confusing way forward.

Generally, due to some samples charging during XPS measurements, the spectra obtained tend to shift to higher BE values. To counter this issue, the spectra need to be calibrated. Here there are a number of approaches. One sets the BE of C–C bonds from adventitious C to ~284.8 eV. One problem with this method is that it relies on C impurities whose BE values are not well agreed upon, and several reports have used values anywhere between 284.5 and 285.0 eV, making reliable calibration difficult.[32] This 0.5 eV difference does not allow accurate calibration.[32] The second method is to add powders of noble metals like Au or Ag to the samples, with well-known BEs.[33] This method has never been used in the MXene literature and is not discussed further.

The third, and highly recommended herein, is aligning the Fermi edge of the spectra to 0 eV. This is an efficient and accurate method of calibration.[32] Therefore the C–C BE should be used for calibration only when the Fermi edge is not sharp or the Ti–C–Ti peak in the C 1s spectra of $Ti_3C_2T_z$ is not at 282.0 eV (see below). In the four fits discussed above, Halim et al.[12] (Fit-I) and Persson et al.[26] (Fit-II) use the Fermi edge for calibration, while Benchakar et al.[27] (Fit-IV) set the Ti–C–Ti peak BE in the C 1s spectra to 281.9 eV. Schultz et al.[17] (Fit-III) do not mention their method of calibration.

Please cite this article in press as: Natu et al., A critical analysis of the X-ray photoelectron spectra of $Ti_3C_2T_z$ MXenes, Matter (2021), https://doi.org/10.1016/j.matt.2021.01.015

Table 5. C 1s BE values of C–Ti–T_z peaks from the literature

MXene	Etching method	BE (eV)	FWHM (eV)	Reference
$Ti_3C_2T_z$	50% HF	282.0	0.6	Halim et al.[12]
	LiF + HCl	282.0	0.6	Ghidiu et al.[15]
	NH_4HF_2	281.9	0.6	Halim et al.[34]
	10% HF etched NaOH treated	282.0	0.6	Halim et al.[35]
	vacuum annealed up to 700°C	282.0	0.6	Persson et al.[26]
Ti_2CT_z	10% HF	281.9	0.6	Halim et al.[12]
Ti_3CN	30% HF	282.1	0.7	Halim et al.[12]
	Average	282 ± 0.06		

Note: values were taken only from studies where the Fermi edge was used for calibration of the XPS spectra.

In the following, we discuss each element separately.

C 1s

As shown in Table 5, the C 1s BE values are quite reproducible between studies. That peak lies at 282.0 ± 0.06 eV. This also implies that the BE of the C atoms in the octahedral sites, *viz.* Ti–C–Ti, are not affected by the type of surface terminations attached during etching in F-ion-containing acids. It also seems to be independent of the M:X ratio, *viz.* n in $Ti_{n+1}X_nT_x$, or the presence of nitrogen, N, in neighboring X sites.

Over the seven studies listed in Table 5, the standard deviation in the BE values is only 0.06 eV. It follows that this BE is an important anchor point that, if not found, suggests problems with the XPS spectra, most likely with calibration and/or the absence of MXenes. Therefore, in cases where the Fermi edge is not sharp enough to use for calibration, we recommend setting the BE in the C 1s spectra to 282.0 eV. It should be noted that this calibration works well with MXenes synthesized in F-containing acids. In recently discovered molten-salt-synthesized MXenes, initial XPS studies suggest the Ti–C–Ti peak BE deviate from 282.0 eV (see below).

The BE of a purely covalent C=C bond is ≈284.5 eV.[36] The Ti–C–Ti BE of 282.0 eV in $Ti_{n+1}C_nT_z$ implies the C atoms are withdrawing electrons from the Ti atoms, which is fairly well established for MXenes at this point.[19] The relationship between the M–C–M component BE and Pauling's electronegativity (EN) of the M in the MXene is plotted in Figure 5 and listed in Table 6. These results indicate that the bond polarity decreases as the EN difference between M and C atoms goes down and that the 282.0 eV value is thus only valid for $Ti_3C_2T_z$ and, even then, as discussed below, only under certain circumstances.

Ti 2p

Before discussing the details of fitting the Ti 2p spectra, several important considerations need to be established. More specifically:

(1) The Ti 2p spectra are always split into two main peaks corresponding to Ti $2p_{3/2}$ and Ti $2p_{1/2}$. Any component fitted to a Ti $2p_{3/2}$ peak should also be used to fit the Ti $2p_{1/2}$ peak. In theory, the area ratio between the two should be exactly 2:1, but, in practice, due to imperfect background subtraction, possible overlapping of satellite peaks, and the Coster-Kronig effect, the area ratios may slightly deviate from expected.[40]
(2) The separation Δ_{Ti2p} between the Ti $2p_{1/2}$ and Ti $2p_{3/2}$ peaks should be consistent for all components assigned to the same material. Here, Δ_{Ti2p} for

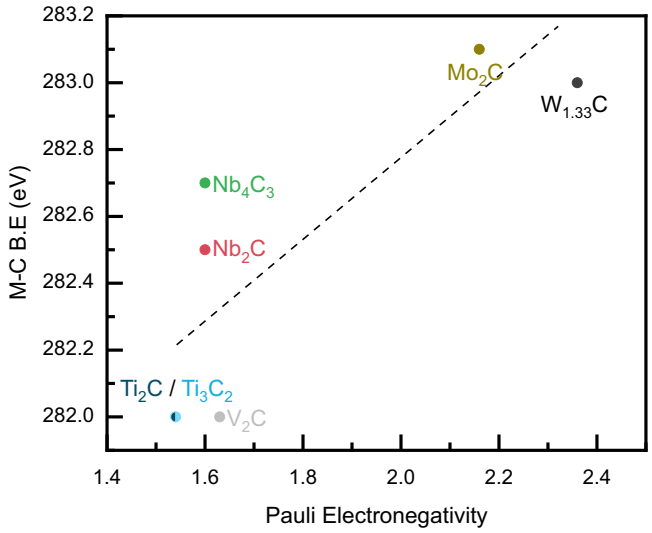

Figure 5. BE of C–M–T_z component in C 1s spectra plotted versus EN of transition metal.
Values were taken only from studies where the Fermi edge was used for calibration of XPS spectra.[12,37–39] Dotted line is a guide to the eye.

$Ti_3C_2T_z$-related peaks is set to 6.1 eV and for oxides and oxyfluorides, it is set to 5.6 eV.

(3) Because MXenes are highly conductive, the component peaks should have asymmetric line shapes instead of the commonly used symmetric Gaussian line shapes. As shown in Figures 6A and 6B, the same Mo 3d spectra of an Mo_2CT_z MXene are fitted using both asymmetric (Figure 6A) and symmetric peaks (Figure 6B). In the latter, an extra, unphysical Mo component is needed to achieve a good fit. This component is not needed when the correct asymmetric peaks are used. Here, Mo_2CT_z was chosen as an example to make this point because only one component is fitted in the Mo 3d spectra, which reduces the ambiguity concerning the number of peaks.

(4) Instead of the more commonly used Shirley background, for $Ti_3C_2T_z$ we suggest using a Tougaard background instead, as it has been shown to give better quantitative results, especially for transition metal-based compounds.[25,41] For consistency, a Tougaard background was used for the C 1s, O 1s, and F 1s spectra as well. Some MXene studies have assumed a linear background. This should be avoided as tit does not have a physical underpinning like the Shirley or Tougaard backgrounds.[25,41] That being said, a more detailed analysis is necessary to understand which background works the best for MXenes as, even under Tougaard or Shirley background, several different variations, like iterated Shirley, 2- or 3-parameter Tougaard, etc., are possible.

Table 6. BE values of C–M–Tz components of various MXenes

MXene composition	BE of C–M–T_z (eV)	Reference
Ti_2CT_z	281.9	Halim et al.[12]
V_2CT_z	282.0	Halim et al.[12]
Nb_2CT_z	282.5	Halim et al.[12]
$Nb_4C_3T_z$	282.7	Halim et al.[12]
Mo_2CT_z	283.1	Halim et al.[37]
$W_{1.33}CT_z$	283.0	Meshkian et al.[38]

Components are as plotted in Figure 5.

Please cite this article in press as: Natu et al., A critical analysis of the X-ray photoelectron spectra of $Ti_3C_2T_z$ MXenes, Matter (2021), https://doi.org/10.1016/j.matt.2021.01.015

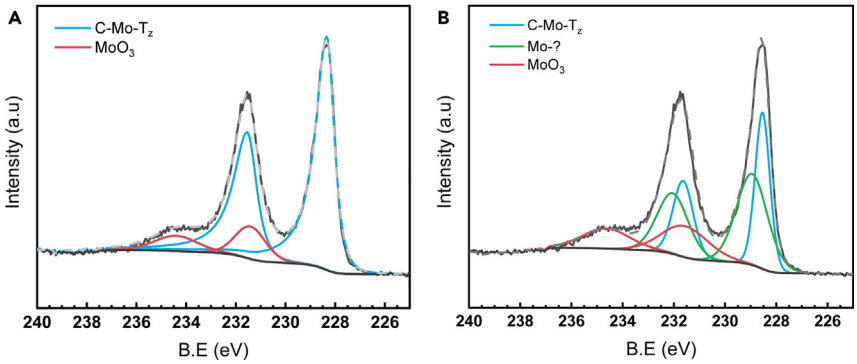

Figure 6. Peak fits of XPS spectra of Mo 3d spectra of Mo_2CT_z MXene

Peak fitting of Mo 3d spectra Mo_2CT_z MXene using (A) asymmetric peaks and (B) symmetric peaks for the C–Mo–T_z component. Raw data were obtained from Intikhab et al.[42] and refit for this figure.

(5) Due to several components being fitted in a broad envelop, currently it is not possible to resolve the full width at half maximum (FWHM) of each component independently. Therefore, we propose to set the FWHM of MXene-related components fits under the Ti $2p_{3/2}$ to be equal. The same for the Ti $2p_{1/2}$; here, we constrained them to have equal FWHM. Note that this does not imply that the FWHM is the same for both; in general, the Ti $2p_{1/2}$ components are broader than their Ti $2p_{3/2}$ counterparts due to the Coster-Kronig effect.

Although the above five points might seem basic to the XPS community, they are at times ignored in the MXene literature, which can lead to false interpretations.

$Ti_3C_2T_z$ VERSUS Ti_2CT_z

In Fit-III, Schultz et al.[17] differentiate Ti bonded to six C atoms and those bonded to only three. They assigned the former with a BE of 455.2 eV. Figures 7A and 7B depict the crystal structures of Ti_2CT_z and $Ti_3C_2T_z$, respectively. The Ti atoms circled in blue, shown in both figures, have identical bonding environments; they are bonded to three C atoms and three Ti atoms (Figure 7C). The Ti atoms in the middle layer of the Ti_3C_2 slab, circled in brown, are surrounded by six C atoms. In other words, these Ti atoms sit in the centers of C octahedra (Figure 7D). So, in principle, there should be two distinct components, with the C–Ti–C atoms having a lower BE than the C–Ti–T_z site since the EN of C is lower than that of O, F, Cl, etc., and should match closely that of Ti in cubic TiC (454.6 eV).[43] More importantly, the C–Ti–C atoms should be absent from the Ti 2p spectra of Ti_2CT_z. However, when we overlay typical Ti 2p spectra of both MXenes (Figure 7E), it is evident that, at lower BEs (to the right of the dashed line), the overlap is excellent. It follows that the C–Ti–C site in $Ti_3C_2T_z$ is indistinguishable from the C–Ti–T_z site by conventional XPS and therefore the assignment of the 455.2 eV peak to the C–Ti–C site in Fit-III and other studies[44–46] is probably wrong. As discussed below, this result may be because the charge on the C atoms in $Ti_3C_2T_z$ is ≈ -2. The deviations between the two Ti spectra at higher BEs are probably due to the difference in the associated –F termination. This comment notwithstanding, more detailed studies using high-resolution synchrotron facilities in tandem with DFT are needed to better understand why the two Ti sites are apparently indistinguishable.

DO THE Ti MXene PEAKS CORRESPOND TO TI OXIDATION STATES OR LOCAL ENVIRONMENTS?

If care is not taken during etching and, more importantly, the storage of $Ti_3C_2T_z$ flakes, they will oxidize, usually to rutile and/or anatase TiO_2.[47,48] If that is the

Please cite this article in press as: Natu et al., A critical analysis of the X-ray photoelectron spectra of $Ti_3C_2T_z$ MXenes, Matter (2021), https://doi.org/10.1016/j.matt.2021.01.015

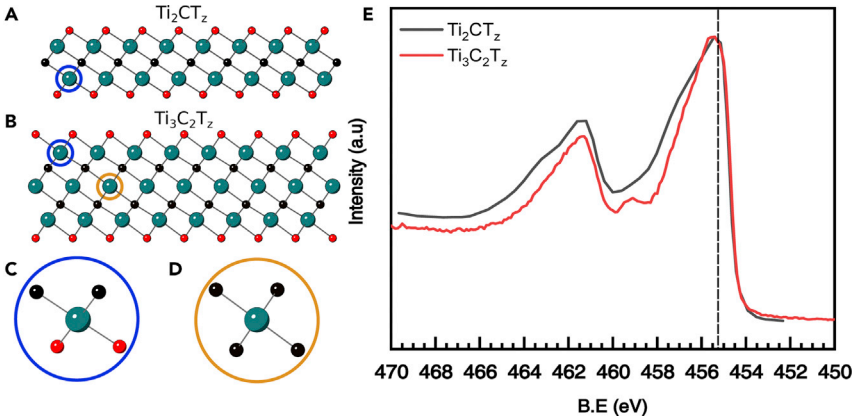

Figure 7. Comparision of crystal structure and Ti 2p XPS spectra of Ti_2CT_z and $Ti_3C_2T_z$ MXenes

(A) Crystal structures of Ti_2CT_z and (B) $Ti_3C_2T_z$ MXenes; (C) and (D) magnified views of Ti atoms circled blue and brown in (A) and (B) with different bonding environments; (E) Ti 2p spectra of Ti_2CT_z (gray) and $Ti_3C_2T_z$ MXene.

case, it is crucial to be able to differentiate the Ti atoms terminated by O atoms and those in separate oxide or oxyfluoride particles. This problem is quite acute if, during etching, the C atoms are replaced by O atoms, as shown by Yoon et al.[49] In this review, we assume that the Ti and C lattice site ratio is preserved at 3:2, respectively. Under harsh etching conditions, that may not be the case. This possibility is not discussed herein, but a good indication that it may be occurring is a $z > 2$.[49,50]

Figure 8 plots the BE of the Ti–O component in the Ti 2p spectra versus the Ti oxidation states in Ti metal (Ti^0), and various Ti oxides, starting with TiO (Ti^{+2}), Ti_2O_3 (Ti^{+3}), and TiO_2 (Ti^{+4}).[29] From this plot, it is reasonable to conclude that the BE differences, ΔBE, between the various Ti oxidation states are more or less constant and equal to ≈1.6 eV.[29] This example was chosen because Ti oxides can be made with a range of stoichiometries with varying oxidation states of Ti atoms and the Ti atoms are always bonded to –O atoms. Therefore, if the type of ligands attached to Ti atoms is kept the same, as in the case here, then ΔBE of Ti $2p_{3/2}$ peaks of the compound should be more or less equal with increasing Ti oxidation states. According to Fit-I and Fit-IV, the ΔBE between the C–Ti^{+1}–T_z and C–Ti^{+2}–T_z components is 0.8 eV, and ΔBE between the C–Ti^{+2}–T_z and C–Ti^{+3}–T_z peaks is 1.4 eV for Fit-I, and 2 eV for Fit-IV.[12,27] However, based on the results shown in Figure 8, the three components should be more or less equally spaced in BE.

Furthermore, based on the X-ray absorption near edge structure (XANES) analysis by Lukatskaya et al.,[19] it was found that the average oxidation state of Ti in $Ti_3C_2T_z$ is ∼+2.4. Based on the fractions obtained in Fit-I (Table 1), if we just consider the first three components, C–Ti^{+1}–O/OH, C–Ti^{+2}–O/OH, C–Ti^{+3}–O/OH, and redistribute the ratios among them, we get new fractions, which are roughly 0.31, 0.33, and 0.35, respectively. The average charge per Ti atom would thus be:

$$0.31 \times 1 + 0.33 \times 2 + 0.35 \times 3 = 2.02 \quad \text{(Equation 1)}$$

This deviation of 0.4 in the Ti oxidation states between Fit-I and the XANES measurements, implies that the fraction of the areas under the first two peaks in Fit-I is overestimated. More importantly, it is highly unlikely that there are Ti oxidation states below +2 in MXene since Ti^{+1} states are unstable.

Regardless of the exact termination chemistries, the molecular weight of $Ti_3C_2T_z$ can be assumed to be ∼200 g/mol. A recent in-depth characterization of $Ti_3C_2T_z$ and

Please cite this article in press as: Natu et al., A critical analysis of the X-ray photoelectron spectra of $Ti_3C_2T_z$ MXenes, Matter (2021), https://doi.org/10.1016/j.matt.2021.01.015

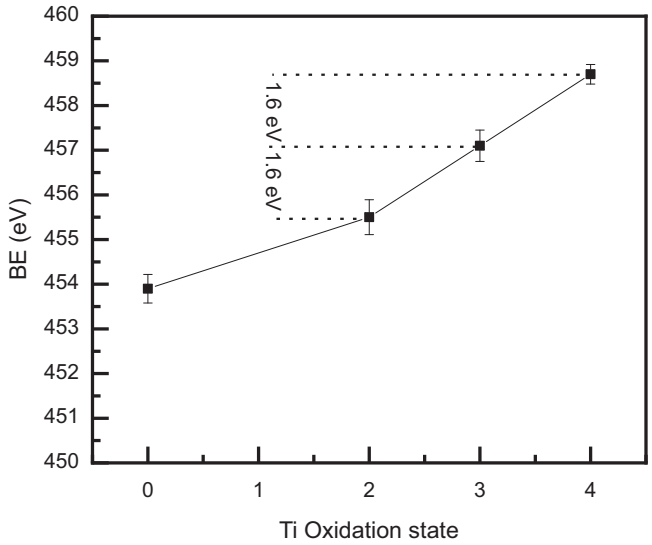

Figure 8. BE of Ti 2p peak BE versus Ti oxidation state in various Ti-oxides
The oxidation state of Ti metal is 0.[29]

Ti_3CNT_z MXenes by Sun et al.[51] concluded, from electron paramagnetic resonance (EPR), that the Ti^{+3} concentration was 7.08×10^{18} atoms/g of $Ti_3C_2T_z$. This translates to <1% Ti^{+3} atoms in $Ti_3C_2T_z$. If that is the case, it follows that both Fit-I and Fit-IV significantly overestimate the Ti^{+3} peak areas.

Therefore, at this juncture, the assumptions made in Fit-II appear to be the best way to fit the Ti 2p XPS spectra in $Ti_3C_2T_z$. In other words, we assign energies to the Ti atoms centered on the following octahedra: C–Ti–O\O\O, C–Ti–F\O\O, C–Ti–F\F\O, and C–Ti–F\F\F, respectively, depicted schematically in Figures 9B–9E. We note in passing that this suggests that the average oxidation state of the C and O atoms are comparable at ≈ -2.

SEPARATIONS BETWEEN THE C–Ti–O/OH AND C–Ti–F PEAKS AND OTHER COMPONENT PEAKS

Figure 10 plots the BEs in the Ti 2p spectra in various TiX compounds, where Ti is in a +3 or +4 oxidation state, versus a normalized EN of X, where X = S, O, F, and Cl. The EN is normalized by multiplying the EN of X atoms by the X/Ti ratio to take the effect of chemistry out of the comparison. The trend is clear: increasing EN of X increases the Ti BEs more or less linearly. Similarly, the slopes are more or less independent of the Ti oxidation states that are +4 for the gray points and +3 for the red ones.[29,30] Another important observation is that, for a given Ti oxidation state, ΔBE between the Ti–F and Ti–O surroundings is constant and around ~2.8–2.9 eV. This is important because it strongly suggests that ΔBE between the C–Ti–O\O\O and C–Ti–F\F\F sites should also be ~2.9 eV. Based on these arguments, if we assign the first Ti 2p peak at 455.0 eV to C–Ti–O\O\O, as done in Fit-II, then the C–Ti–F\F\F peaks should be around 2.9 eV higher at ≈458 eV. The C–Ti–O\O\F and C–Ti–O\F\F, on the other hand, should be ≈1 eV apart at 456 eV and 457 eV, respectively.

To confirm that interpolations from Figure 10 are meaningful, the Ti 2p BE value of $TiOF_2$[52,53] is calculated from the gray curve and found to be 459.6 eV, which matches quite well with the experimental BE of 459.5 eV (blue star in Figure 10), found in the

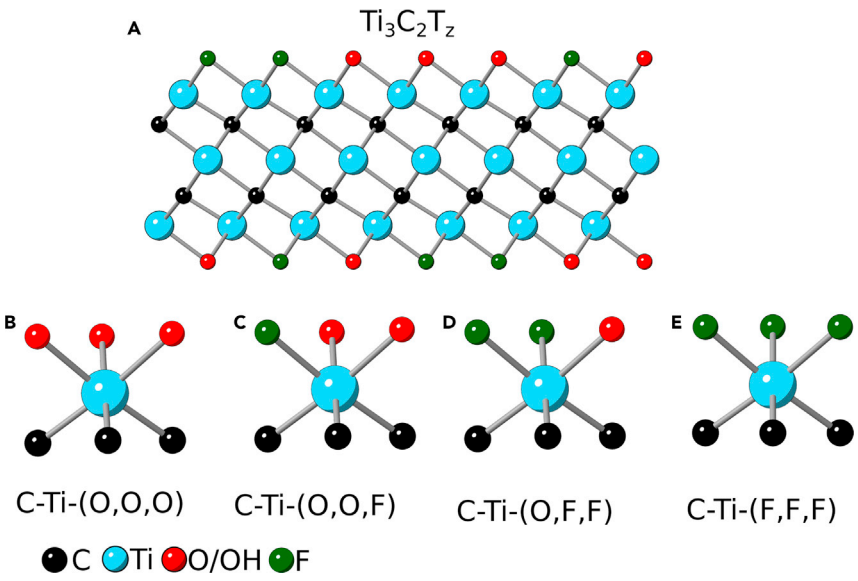

Figure 9. Possible surface termination combinations around surface Ti atoms

(A) Crystal structure of $Ti_3C_2T_z$; surface Ti atoms terminated by, (B) 3 O atoms, (C) 1 F and 2 O atoms, (D) 2 F and 1 O atom, and (E) 3 F atoms.

literature.[52,53] A similar exercise for TiOCl gives a value, based on Figure 10, of 457.8 eV, which again is in good agreement with the value of 457.9 eV reported in the literature[54] (green star Figure 10). These arguments strongly support the placement of C–Ti–F\F\F peak 2.9 eV *higher* than its O counterpart.

Finally, it should be noted that –OH terminations are also found on MXene surfaces (see below). Here we assume they are indistinguishable from their O counterparts in the Ti 2p spectra.[55,56] Henceforth, this fitting protocol will be referred to as Fit-V.

Fit-V

In addition to the arguments made above, the following constraints were applied in our fit:

(1) Similar to Fit-II, the ΔTi_{2p} for all MXene peaks was kept constant at 6.1 eV.
(2) Based on XPS studies of TiO_2, for the oxide peaks, Δ_{Ti2p} was set to 5.6 eV.[55]
(3) The peak shape used for the MXene components is asymmetric and similar to that used by Biesinger et al.,[29] as described in their XPS fittings of Ti metal[1,29] (Biesinger confirmed that asymmetric lines can also be used for fitting the Ti–C component in cubic TiC [personal communication]. The sample fit of cubic TiC according to Biesinger et al.[29] can be found on his website at http://www.xpsfitting.com/2008/10/titanium-carbide.html). Symmetric Gaussian peaks, on the other hand, were used to fit the oxide contributions.
(4) As discussed earlier, a Tougaard background was assumed for fitting all core-level spectra.
(5) The FWHM of all C–Ti–Tz peaks fitted under the Ti $2p_{3/2}$ peak were constrained to be equal. Similarly, all C–Ti–T_z peaks fitted under the Ti $2p_{1/2}$ peak were constrained to be equal.

OXIDES IN $Ti_3C_2T_z$ MXene

It is commonly assumed that, when Ti-containing MXenes oxidize, they form TiO_2. A careful perusal of these oxidation studies[27,47] shows that clear oxide peaks emerge

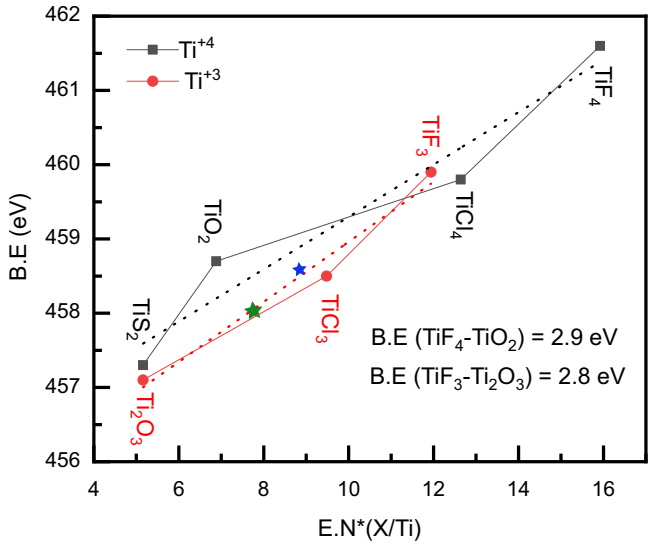

Figure 10. BE of Ti–X (X = S, O, F, Cl) component in the Ti 2p spectra versus normalized EN of X atom

Gray points join Ti^{+4} compounds; red, Ti^{+3}.[29,30] Blue star marks BE of $TiOF_2$ and green marks that of TiOCl.[52–54]

at BEs between 459.0 and 459.5 eV. These values are higher than the ~458.6 eV values reported for pure TiO_2 oxides.[29] Based on the arguments made in Figure 10, it is reasonable to assume that the TiO_2 formed is not pure, but is rather doped with some F atoms and therefore those peaks should be labeled as $TiO_{2-x}F_{2x}$ instead of TiO_2. Although it is difficult to find the exact value of x, a rough estimate can be calculated by interpolating the BE values from the gray curve shown in Figure 10.

Based on all the above points, we refit the Ti 2p data by Benchakar et al.[27] for $Ti_3C_2T_z$, etched in 10% hydrofluoric acid, HF, according to Fit-V, and the peak fits are shown in Figure 11. The corresponding BE values for each component are listed in Table 7.[27]

MXene SYNTHESIZED IN MOLTEN SALTS

Recently, Li et al.[13] synthesized $Ti_3C_2T_z$ MXenes where T was Cl using a molten salt synthesis approach. In their XPS fits, they used symmetric instead of asymmetric peaks, which resulted in an extra set of peaks. As discussed above, the extra peak is probably an artifact of using symmetric peaks. Further, they calibrated their spectra using the adventitious C peak, which might not lead to accurate results. We refit their raw data using the assumptions made for Fit-V, as shown in Figures 12A and 12B, and Table 8. Recently, Lu et al.[57] found that MXene surfaces synthesized in molten $ZnCl_2$ salts are completely saturated by Cl terminations. Based on these observations there should be only one set of peaks corresponding to C–Ti–Cl\Cl\Cl. Unfortunately, as the Fermi edge was not scanned, so we had to calibrate the spectra by setting the Ti–C–Ti peak to 282.0 eV. Doing so resulted in a C–Ti–Cl\Cl\Cl BE of 454.8 eV, which is unlikely since that is equal to the BE in the parent MAX.[58] Intriguingly, and for reasons that are unclear at this time, when we etched Ti_3AlC_2 in a non-aqueous solution, where the terminations were quite F rich, the Ti–C–Ti peak was found at 282.0 eV.[59]

Please cite this article in press as: Natu et al., A critical analysis of the X-ray photoelectron spectra of $Ti_3C_2T_z$ MXenes, Matter (2021), https://doi.org/10.1016/j.matt.2021.01.015

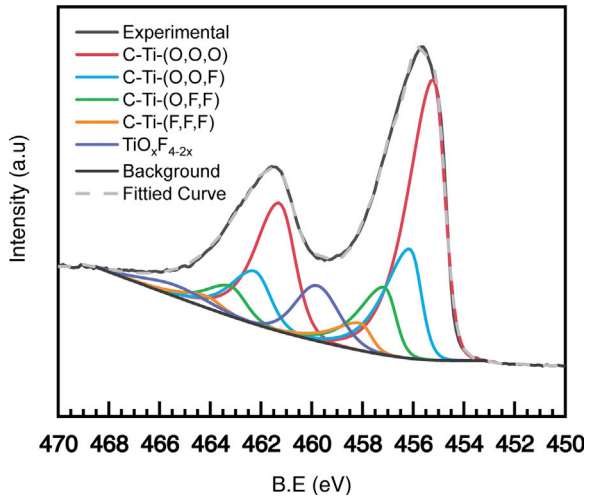

Figure 11. XPS spectra of Ti 2p region fit according to Fit-V

Raw data used obtained from Benchakar et al.[27] were recorded from $Ti_3C_2T_z$ etched from Ti_3AlC_2 in 10% HF.

Similarly, we refit the XPS results of Kamysbayev et al.[14] (Figures 12C–12H), based on the assumption that the MXene surface is saturated with only one type of termination. It should be noted here that Li et al.[13] used a C–C BE of 284.6 eV for calibration, while Kamysbayev et al.[14] used a BE of 284.8 eV. This is a good example of why using C–C bond BE for calibration is not recommended.

Referring back to Figures 12C–12H. Here again, because the Fermi edge was not scanned, we set the Ti–C–Ti peak to 282.0 eV for calibration purposes. In the case of $Ti_3C_2Br_2$ (Figures 12C and 12D), the BE of the C–Ti–Br\Br\Br bond was found to be 454.8 eV, which is coincidentally equal to that C–Ti–Cl\Cl\Cl bond of $Ti_3C_2Cl_2$. Attaching highly electronegative Cl or Br terminations should shift the BE to higher, rather than lower, values. What both sets of results suggest is that the Ti–C–Ti peak in MXenes synthesized in molten salts can no longer be assumed to be at 282.0 eV.

In the case of $Ti_3C_2Te_z$ (Figures 12E and 12F), the C–Ti–Te\Te\Te BE was found to be 455.0 eV, which is comparable with the C–Ti–O\O\O peak of $Ti_3C_2T_z$ synthesized in F-containing acids. Even though Te is less electronegative than O, the BE of the first peak does not shift below 455.0 eV. Here again, this conclusion probably stems from the Ti–C–Ti peak not being at 282.0 eV. The C–Ti–() peak, where () represents an unterminated Ti bond (Figures 12G and 12H), in the unterminated MXene samples was at 454.9 eV (Table 8), which is slightly lower than the first peak of C–Ti–O\O\O at 455.0 eV found in regular MXene. This shift of BE to lower energy is expected as electron-withdrawing surface terminations are removed from the surface. In the case of $Ti_3C_2()$, a second MXene peak at 456.7 eV (Table 8) was added to achieve a good fit. What this peak physically corresponds to is currently unclear.

These comments notwithstanding, more work needs to be carried out to examine and better understand these chemical shifts. Having a well-calibrated energy scale is crucial and highly recommended.

O 1s

The O 1s spectra of fits I–IV are all different. Fit-I has five component peaks: the lowest energy peak at 529.9 eV is ascribed to TiO_2; the next two peaks at 531.2

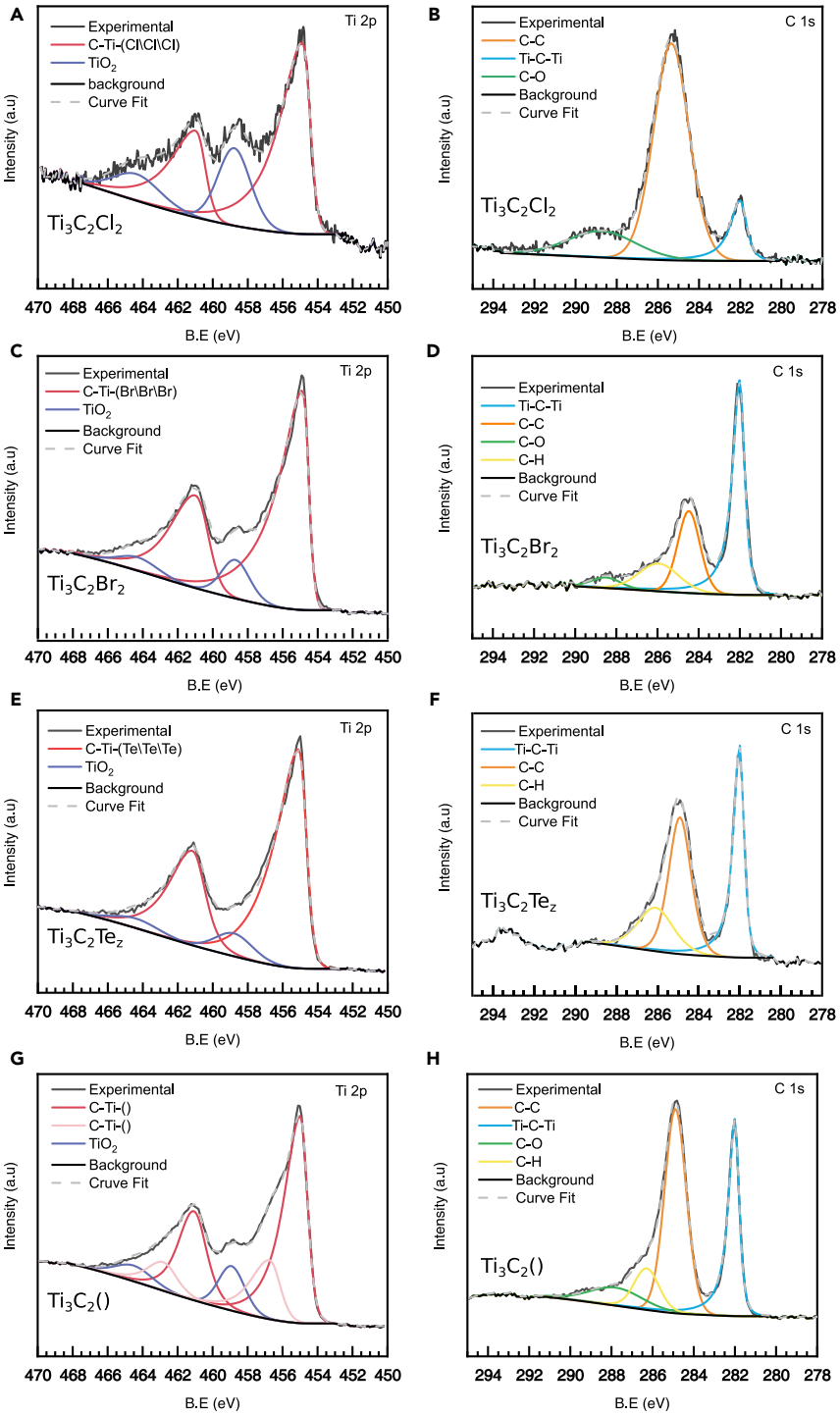

Figure 12. XPS spectra of Ti 2p and C 1s region fit according to Fit-V

Raw data obtained from Li et al.[13] and Kamysbayev et al.[14] were recorded from $Ti_3C_2T_z$ powders etched in molten salt baths starting with Ti_3AlC_2 at 550°C in the case of $Ti_3C_2Cl_2$ and 650°C in for the remaining compositions. (A and B) Ti 2p and C 1s spectra of $Ti_3C_2Cl_2$; (C and D) Ti 2p and C 1s spectra of $Ti_3C_2Br_2$; (E and F) Ti 2p and C 1s spectra of Ti_3C_2Te; (G and H) Ti 2p and C 1s spectra of $Ti_3C_2()$, where () refers to non-terminated surfaces.

Please cite this article in press as: Natu et al., A critical analysis of the X-ray photoelectron spectra of $Ti_3C_2T_z$ MXenes, Matter (2021), https://doi.org/10.1016/j.matt.2021.01.015

Table 7. Summary of XPS peak fittings of Ti 2p spectra of $Ti_3C_2T_z$ synthesized by etching Ti_3AlC_2 MAX in 10% HF solution

Region	BE (eV)	FWHM (eV)	Fraction	Assigned to
Ti $2p_{3/2}$ ($2p_{1/2}$)	455.1 (461.1)	1.1 (1.5)	0.53	C–Ti–(O\O\O)
	456.0 (462.1)	1.1 (1.5)	0.22	C–Ti–(O\O\F)
	457.0 (463.1)	1.1 (1.5)	0.11	C–Ti–(O\F\F)
	457.9 (464.0)	1.1 (1.5)	0.04	C–Ti–(F\F\F)
	459.6 (465.2)	2.0 (3.0)	0.10	$TiO_{2-x}F_{2x}$

Components were fit according to Fit-V as shown in Figure 11. BE and FWHM values of the Ti $2p_{3/2}$ peaks are listed in columns 2 and 3, respectively. Respective numbers for Ti $2p_{1/2}$ peaks are shown in brackets. Spectra obtained from Benchakar et al.[27]

eV and 532.0 eV are assigned to C–Ti–O and C–Ti–OH, respectively. The peaks at 523.8 and 533.8 eV are allocated to alumina and adsorbed water respectively.

Persson et al.[26] (Fit-II) claim that –OH terminations are not present on the MXene surfaces and the peak ascribed to C–Ti–OH in Fit-I is actually that of –O terminations that occupy bridging sites (see Figures 2 and 3E). They argued that, if the peak at 532.0 eV was due to OH, then the observed intensity loss of this peak, with increasing temperature, should reduce the total area under the O 1s curve during annealing, which is not observed. From there they conclude that the changes in peak intensities observed are due to a rearrangement of surface O atoms from bridging sites to A sites (Figure 2).

Table 8. Summary of XPS peak fittings of Ti 2p spectra of as-synthesized $Ti_3C_2T_z$ obtained by etching Ti_3AlC_2 in molten salt baths

Sample	Region	BE (eV)	FWHM (eV)	Fraction	Assigned to
$Ti_3C_2Cl_2$	Ti $2p_{3/2}$ ($2p_{1/2}$)	454.8 (460.9)	1.1 (1.3)	0.73	C–Ti–Cl\Cl\Cl
		458.7 (464.3)	2.2 (3.2)	0.27	TiO_2
	C 1s	282.0	0.8	0.12	Ti–C–Ti
		285.3	2.0	0.77	C–C
		288.9	2.5	0.11	C–O
$Ti_3C_2Br_2$	Ti $2p_{3/2}$ ($2p_{1/2}$)	454.8 (460.9)	0.9 (1.7)	0.88	C–Ti–Br\Br\Br
		458.7 (464.3)	1.9 (2.7)	0.12	TiO_2
	C 1s	282.0	0.6	0.52	Ti–C–Ti
		284.5	1.3	0.27	C–C
		285.9	2.3	0.16	C–H
		288.5	1.7	0.05	C–O
Ti_3C_2Te	Ti $2p_{3/2}$ ($2p_{1/2}$)	455.0 (461.1)	1.0 (1.7)	0.90	C–Ti–Te
		458.8 (464.4)	2.5 (3.0)	0.10	TiO_2
	C 1s	282.0	0.5	0.40	Ti–C–Ti
		285.0	1.3	0.40	C–C
		286.0	2.0	0.20	C–H
$Ti_3C_2()$	Ti $2p_{3/2}$ ($2p_{1/2}$)	454.9 (461.0)	1.0 (1.7)	0.65	C–Ti–()
		456.7 (462.8)	1.4 (1.8)	0.23	C–Ti–()
		458.9 (464.5)	1.7 (2.5)	0.12	TiO_2
	C 1s	282.0	0.5	0.30	Ti–C–Ti
		284.9	1.2	0.47	C–C
		286.3	1.4	0.12	C–H
		287.8	3.0	0.11	C–O

The components were fit according to Fit-V as shown in Figure 12. BE and FWHM values of the Ti $2p_{3/2}$ peaks are listed in columns 2 and 3, respectively. Respective numbers for Ti $2p_{1/2}$ peaks are shown in brackets. Spectra obtained from Li et al.[13] and Kamysbayev et al.[14]

Please cite this article in press as: Natu et al., A critical analysis of the X-ray photoelectron spectra of $Ti_3C_2T_z$ MXenes, Matter (2021), https://doi.org/10.1016/j.matt.2021.01.015

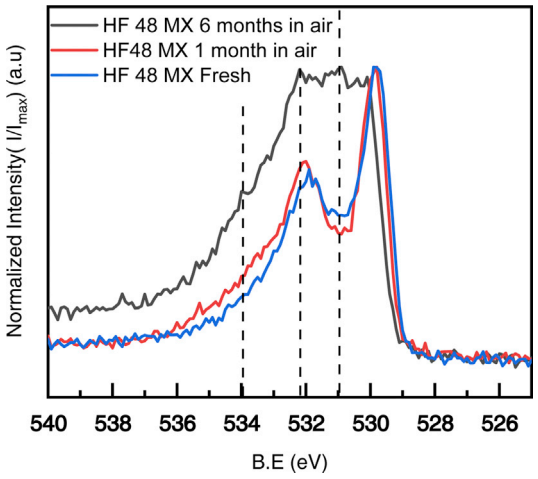

Figure 13. O 1s spectra of fresh $Ti_3C_2T_z$ films immediately after synthesis (blue) and after aging the same sample for 1 month (red) and 6 months (gray)

However, Seredych et al.,[60] in their thermogravimetric analysis, coupled with gas mass spectroscopy (TGA-MS) studies of various MXene under flowing He gas, showed that, upon heating, the F atoms desorb from the MXene surface in the form of HF and not F_2 molecules.[60] If that is the case, then the –OH terminations can be converted to –O by the loss of H to HF formation. In such a scheme, the total O content would remain unchanged, as observed. Although this is just a hypothesis to possibly explain the lack of O 1s area change by Persson et al.,[26] more work is needed to better understand this phenomenon.

Moreover, recent NMR and neutron scattering studies have proven the presence of –OH terminations.[20,51,61] Another important point to note is that vacuum annealing experiments by Persson et al.[26] were carried out in ultrahigh vacuum that, in principle, allow for O re-arrangements. However, to understand the true nature of the O/OH terminations, the samples need to be re-exposed to air and water to saturate the lattice sites left unterminated after –F desorption and the sample should be rescanned.

Fit-III is similar to Fit-II, but instead of two possible crystallographic sites proposed in Fit-II (Figure 2D), three different possible sites are proposed (Figures 3A and 3H). Fit-IV uses a mix of Fit-I and Fit-II and ascribed the peaks at 529.7 and 531.2 eV to bridging and A-site O, while the peak at 532.0 eV was assigned to the C–Ti–OH bond.

Fit-I assigns the peak at 529.9 eV to $TiO_2/TiO_{2-x}F_{2x}$, while in Fit-IV that peak is fitted at 530.6 eV. They cannot both be correct. To determine which of these is correct, the data by Benchakar et al.[27] were replotted and the O 1s spectra of freshly synthesized MXene films obtained after etching Ti_3AlC_2 in 48% HF and their subsequent aging in the ambient atmosphere for 1 and 6 months were overlaid in Figure 13.[27] From these results it is obvious that after 6 months a clear peak appears at a BE of ~530.8 eV, implying that the oxide peak assignment in Fit-IV is correct. Moreover, in their study, Benchakar et al.[27] confirmed that peak intensity increases with the fraction of $TiO_{2-x}F_x$ in the Ti 2p region, as shown by the preparation of partially oxidized $Ti_3C_2T_z$ using a FeF_3/HCl etching agent (Figure 4). This attribution was adopted in our Fit-V.

Based on these observations, it is clear that fitting O 1s spectra in $Ti_3C_2T_z$ is not trivial due to multiple overlapping contributions from surface terminations, oxides, and

Please cite this article in press as: Natu et al., A critical analysis of the X-ray photoelectron spectra of $Ti_3C_2T_z$ MXenes, Matter (2021), https://doi.org/10.1016/j.matt.2021.01.015

Table 9. Chemistries of $Ti_3C_2T_z$ samples all obtained by etching Ti_3AlC_2 in 48% HF

Method	Formula	O:OH:F	T_z Total z	T_z Charge total	Reference
XPS[a]	$Ti_3C_2O_{0.3}(OH)_{0.02}(OH/H_2O_{ads})_{0.3}F_{1.2}$	1:0.07:4	1.52 (1.82)	1.82 (2.12)	Halim et al.[12]
XPS[b]	$Ti_3C_{2.03}O(i)_{0.43}O(ii)_{0.06}(OH)_{0.3}F_{1.34}$	1:0.6:2.7	2.13	2.62	Benchakar et al.[27]
NMR[c]	$Ti_3C_2O_{0.84}(OH)_{0.06}F_{0.25}$	1:0.07:0.3	1.15	2.0	Hope et al.[20]
PDF[d]	$Ti_3C_2O_{0.1}(OH)_{0.8}F_{1.1}$	1:8:11	2.0	2.1	Wang et al.[62]

Charge total is calculated by assuming charge on O = −2 and on OH and F = −1. Chemistries reported by XPS herein are ones reported in the original work.

[a]In Ref.,[12] Halim et al. calculated values in parenthesis assuming all the H_2O as OH; the values outside the parenthesis are assuming otherwise.

[b]In Ref.,[27] Benchakar et al. fit two sites for O terminations denoted (i) and (ii) for calculation of T_z; both have been added.

[c]In Ref.,[20] Hope et al. assumed a charge total of T_z equal to +2 and back-calculated the stoichiometry.

[d]In Ref.,[62] Wang et al. assumed z = 2 and back-calculated the stoichiometry.

hydroxides. Moreover, the impurities from adventitious C and other organics contribute to the O 1s spectra as well and their contribution cannot be determined at this point. Therefore, more work is required to better understand the O 1s spectra.

F 1s

Fit-I, Fit-III, and Fit-IV all assign only one peak to F terminations with a BE ~ 685.0 eV. Fit-II fits two peaks corresponding to C–Ti–F and C–Ti–(O, F) at 684.5 and 685.4 eV respectively. Depending on the etching and processing conditions, impurities like AlF_3 and $TiO_{2-x}F_{2x}$, are also fit under the F 1s spectra. However, since F is the most EN element, the chemical shifts in its XPS spectra are small, rendering the quantification of impurities difficult. Furthermore, the choice of asymmetry for the C–Ti–F peaks will also influence the quantification of any impurity peaks.

QUANTIFICATION

As discussed above, it is not trivial to quantify the surface terminations of $Ti_3C_2T_z$ flakes using XPS. What renders the problem even more intractable is that the results obtained from different characterization techniques, on nominally comparable samples, are not close. This is best seen by a perusal of the chemistries listed in Table 9, on samples obtained by etching Ti_3AlC_2 powders in 48% HF at room temperature (RT). The results of XPS analyses[12,27] are compared with those obtained by NMR[20] and neutron pair distribution function (PDF) analysis.[62] The final chemistries (column 2 in Table 9) are quite different. From Table 9 it is also clear that there are discrepancies not only in the chemistries between the various XPS studies but also between the various techniques. Referring to column 3 in Table 9, the O:OH ratios vary anywhere from 0.07 to 8, and the O:F ratio varies from 0.3 to 11. Ideally, all techniques should yield comparable chemistries. The fact that they do not implies that much more work is needed in this domain. These large deviations imply that either some of these techniques cannot be used to properly quantify the termination chemistries, or more in-depth studies are required to shed light on these discrepancies. In Figure 14, we refit the results of Benchakar et al.[27] for Ti_3AlC_2 etched in 10% HF using Fit-V. The results are summarized in Table 10. The C 1s spectra were fit with one asymmetric peak at 282.0 eV corresponding to C atoms centered in Ti octahedra. The other C 1s peaks were ascribed to adventitious C.

Please cite this article in press as: Natu et al., A critical analysis of the X-ray photoelectron spectra of $Ti_3C_2T_z$ MXenes, Matter (2021), https://doi.org/10.1016/j.matt.2021.01.015

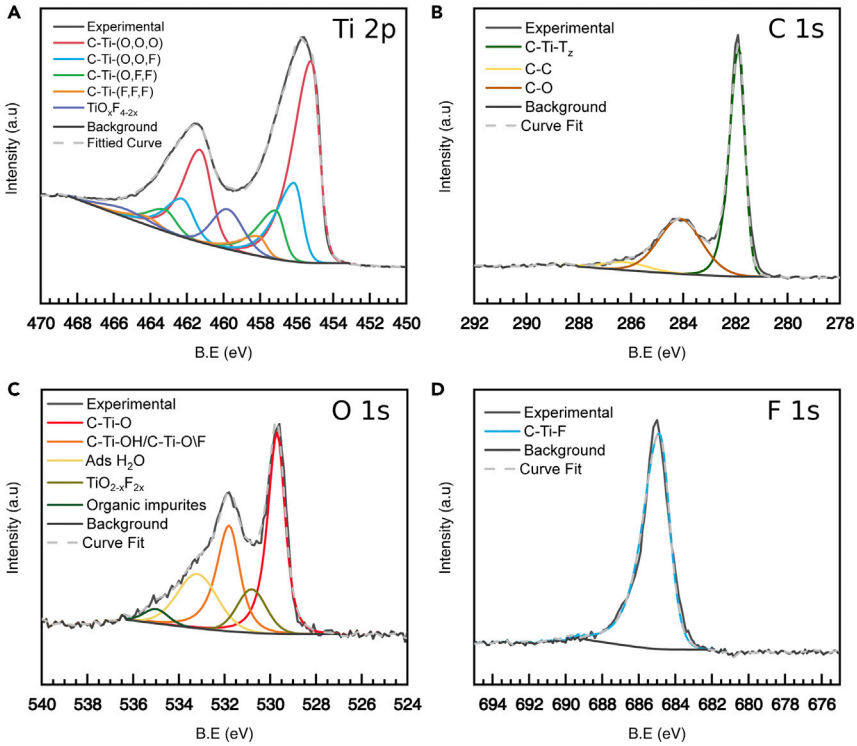

Figure 14. XPS spectra of $Ti_3C_2T_z$ MXene fit according to Fit-V

Fit-V of XPS spectra of $Ti_3C_2T_z$ obtained after etching Ti_3AlC_2 in 10% HF, (A) Ti 2p, (B) C 1s, (C) O 1s and, (D) F 1s regions. Raw data obtained from Benchakar et al.[27]

In the O 1s spectra, the first peak at 529.8 eV was ascribed to C–Ti–O\O\O. The peak at ~532.0 eV is ascribed to the C–Ti–OH bond in Fit-I and Fit-IV and to a C–Ti–O/F bond in Fit-II, where O/F corresponds to the O co-adsorbed with F atoms. Moreover, by coupling XPS and Raman spectroscopy and by comparing $Ti_3C_2T_z$ etched with HF10% and HF48%, which in turn allowed for a variation of the OH/O ratios, Benchakar et al.[27] show that this peak can, with a large degree of certainty, be attributed to C–Ti–OH. Nevertheless, a contribution of the C–Ti–O/F bond in this peak cannot be excluded. Therefore, in Fit-V we assume that the 532.0 eV peak is probably a convolution of C–Ti–OH and C–Ti–(O, F) moieties. The 530.8 eV peak was ascribed to O in $TiO_{2-x}F_{2x}$ (Figures 13 and 14).[53]

The F 1s spectra were fitted with only one asymmetric peak at 684.9 eV. Given that the BE of the F 1s peak in $TiO_{2-x}F_{2x}$ is also ~685.0 eV,[52,53] it is currently not possible to deconvolute the peak.

For the quantification shown in Table 10, a few assumptions were made:

(1) The BE of the $TiO_{2-x}F_{2x}$ peak in the Ti 2p spectra was constrained between 459.0 and 460.0 eV. We further assume x = $^1/_2$. This implies the oxide chemistry is $TiO_{1.5}F$. It should be noted that the BE of $TiOF_2$ shown in Figure 10 was obtained from prior work where the presence of $TiOF_2$ was also confirmed by XRD. In the case of oxide formation due to oxidation of $Ti_3C_2T_z$, XPS indicates a BE closer to $TiOF_2$. XRD measurements, however, indicate the presence of rutile or anatase TiO_2.[47] Prior work by Czoska et al.[64] on F-doped TiO_2 found that some F atoms can play two roles: some replace O atoms in the TiO_2

Please cite this article in press as: Natu et al., A critical analysis of the X-ray photoelectron spectra of $Ti_3C_2T_z$ MXenes, Matter (2021), https://doi.org/10.1016/j.matt.2021.01.015

Table 10. Summary of XPS peak fittings based on Fit-V for MXene synthesized using 10% HF

Region	BE (eV)	FWHM (eV)	Fraction	Assigned to
Ti $2p_{3/2}$ ($2p_{1/2}$)	455.1 (461.1)	1.1 (1.5)	0.53	C–Ti–(O\O\O)
	456.0 (462.1)	1.1 (1.5)	0.22	C–Ti–(O\O\F)
	457.0 (463.1)	1.1 (1.5)	0.11	C–Ti–(O\F\F)
	457.9 (464.0)	1.1 (1.5)	0.04	C–Ti–(F\F\F)
	459.6 (465.2)	2.0 (3.0)	0.10	$TiO_{2-x}F_{2x}$
C 1s	282.0	0.6	0.74	Ti–C–Ti
	284.4	1.9	0.20	C–C
	286.5	1.5	0.06	C–O
O 1s	529.8	0.9	0.51	C–Ti–O
	532.0	1.0	0.18	C–Ti–OH/C–Ti–O/F
	530.8	2.0	0.23	$TiO_{2-x}F_{2x}$
	533.4	1.5	0.08	Adsorbed H_2O
F 1s	684.9	1.1	1	C–Ti–F/$TiO_{2-x}F_{2x}$

BE and FWHM values of the Ti $2p_{3/2}$ peaks are listed in columns 2 and 3, respectively. Respective numbers for Ti $2p_{1/2}$ peaks are shown in brackets. Peak fittings as shown in Figure 14.

lattice and others replace surface hydroxyl groups. We believe a similar phenomenon also occurs on the surface of TiO_2 formed on MXene surfaces because XPS indicates a higher F content compared with a bulk analysis by XRD. Therefore, we assume an approximate stoichiometry of $TiO_{1.5}F$. Further, depending on the etching condition used, Mashtalir et al.[65] and Benchakar et al.,[6] from their XRD and Raman spectroscopy analysis, respectively, also observed the formation of $TiOF_2$ and/or $TiO_{2-x}F_{2x}$ in MXene samples. It should be noted that, since TiO_2 is a semiconductor, its corresponding peaks might shift to higher BE due to local charging, band bending, etc. However, previous XPS studies of TiO_2 on metallic substrates[66,67] found that the BE of the Ti $2p_{3/2}$ peak ascribed to TiO_2 was below 459.0 eV. It is thus reasonable to assume here, given the conductive nature of $Ti_3C_2T_z$, that the TiO_2 peaks should *not* move to higher BE and that the shifts are solely due to F on the surface and/or the bulk of the oxide. However, to confirm these conjectures, more detailed, and preferably *in situ*, oxidation studies of $Ti_3C_2T_z$ should be carried out.

(3) The BE of the $TiO_{2-x}F_{2x}$ peak in the O 1s spectra was assumed to be 530.8 eV (according to the O 1s discussion based on Figure 13). The area was constrained such that the Ti:O ratio in the oxide stoichiometry was 1:1.5 based on a $TiO_{1.5}F$ formula.

(4) Since we assume that the $TiO_{2-x}F_{2x}$ peak overlaps with the C–Ti–F peak in the F1s region, the area of the oxide peak was subtracted from the total peak area. The oxide peak area subtracted was constrained such that the Ti:F ratio in oxide stoichiometry was 1:1, again based on the assumed $TiO_{1.5}F$ formula.

(5) Minimal impurities were assumed. Other than adventitious C and $TiOF_2$ no other impurities were taken into consideration during fitting.

Based on these fits, the chemical formulae obtained (Table 11) agree well with two general well-established structural constraints. The first is that the Ti:C ratio of MXene is roughly 3:2. The second is that z in $T_z \sim 2$. The latter is an excellent assumption since this is the value one obtains if one were to fill the close-packed sites on the Ti surfaces. In other words, it is the value one would obtain if every termination atom is bonded to three Ti atoms. DFT calculations have shown that the energy of the system increases rapidly for $z > 2$.[68] Values of $z > 2.5$ suggest that termination atoms, especially O, are substituting for C atoms in the Ti_3C_2 layers.[49]

Please cite this article in press as: Natu et al., A critical analysis of the X-ray photoelectron spectra of $Ti_3C_2T_z$ MXenes, Matter (2021), https://doi.org/10.1016/j.matt.2021.01.015

Table 11. MXene chemistries calculated after applying Fit-V to $Ti_3C_2T_z$ spectra obtained from Ti_3AlC_2 powders etched in various media and conditions indicated in column 1

			Charge total of Tz		
Etchant	Chemistry	z (moles)	Fit-IV Benchakar et al.[27]	Assuming all O_F	Assuming all OH
HF- 48%	$Ti_3C_{1.94}O_{0.39}(O_F/OH)_{0.25}F_{1.5}$	2.14		−2.8	−2.53
	$Ti_3C_{2.03}O_{0.49}(OH)_{0.30}F_{1.34}$[a]	2.13	−2.62		
HF - 10%	$Ti_3C_{2.1}O_{0.81}(O_F/OH)_{0.20}F_{0.89}$	1.9		−2.91	−2.71
	$Ti_3C_{2.08}O_{1.04}(OH)_{0.19}F_{0.61}$[a]	1.84	−2.88		
LiF + HCl (60°C)	$Ti_3C_{2.1}O_{0.98}(O_F/OH)_{0.15}F_{0.8}$	1.93		−3.07	−2.91
	$Ti_3C_{1.86}O_{1.0}(OH)_{0.16}F_{0.70}$[a]	1.86	−2.86		
LiF + HCl (RT)	$Ti_3C_{2.0}O_{0.85}(O_F/OH)_{0.30}F_{0.94}$	2.09		−3.24	−2.94
	$Ti_3C_{1.94}O_{0.94}(OH)_{0.17}F_{0.75}$[a]	1.86	−2.80		

All raw data obtained from Ref.[27] Total charge on terminations is calculated assuming O = −2 and OH and F = −1. O_F stands for O co-absorbed with F. As we cannot differentiate between OH and O_F in Fit-V in column 5, we assume all the 532.0 eV peaks in O 1s to be only O_F, while in column 6 we assume it be all OH while calculating the charge total of T_z. For Fit-IV this differentiation is not made so charge total is given in column 4.

[a]Obtained using Fit-IV on results published in Ref.[27]

Values of $z < 2$ would imply the presence of bare Ti bonds, which is impossible given its reactivity. Even in ultrahigh vacuum, Ti surfaces are rapidly covered in a layer of oxygen, let alone ambient atmospheres. If any XPS analysis results in $z << 2$, that should be taken as a large red flag that the analysis is seriously flawed. These constraints are important and deviations from these values suggest either problems with the fits and/or very unusual processing/storing protocols. Therefore, Fit-V can also be used for the overall quantification of surface terminations. $Ti_3C_2T_z$ etched in 48% HF has nearly double the F content compared with MXene synthesized using milder etching methods (Table 11). Also, the charge calculated based on T_z was slightly lower in MXene synthesized using 48% HF compared with MXene synthesized using milder etching methods. For the latter, the average charge of T_z is between −2.9 and −3.2. At −2.5 to −2.8, it is slightly lower in samples etched in 48% HF. Based on these results, if we assume an average T_z charge of 3.2 considering all the contribution under the 532.0 eV in O 1s to be from the C–Ti–(O, F) and assuming the Ti oxidation state to be +2.4, we can calculate the oxidation state of C to be ≈ –1.9. Doing a similar calculation but instead ascribing the peak at 532.0 eV completely to C–Ti–OH, and assuming an average T_z charge of 2.9, the oxidation state of C is −2.15. In other words, in both cases, the average oxidation of C is ≈ −2. If that is the case, it is not surprising that it is difficult to differentiate in the Ti 2p spectra between the central Ti atoms and those near surfaces terminated by O\O\O.

The average depth of analysis using XPS is generally around 5–10 nm.[25,63] Unlike bulk materials that can be assumed to be homogeneous for nanomaterials like MXene that are only 1 nm thick, the XPS quantification is averaging over several MXene flakes. For example, assuming a 200-μm spot size of the X-ray beam and a probing depth of 10 nm gives us average quantification over 10^6 MXene flakes. Therefore, we are not collecting signals from just the surface terminations but also from the core of each flake; the interlayer intercalated species like cations and water molecules; and from impurities like oxides, etching residues, etc. Also, the subsurface photoelectrons will have higher scattering lengths compared with the ones on the surface, and subsurface MXenes flakes

Please cite this article in press as: Natu et al., A critical analysis of the X-ray photoelectron spectra of $Ti_3C_2T_z$ MXenes, Matter (2021), https://doi.org/10.1016/j.matt.2021.01.015

will tend to show slightly different chemistry than the MXene flakes on the surface of the sample due to this artifact. Therefore because of these problems, it is difficult to obtain exact chemistries of bulk MXene samples, but rough estimations can be obtained via our proposed fittings.

CONCLUSIONS

In this work, we compare and contrast four methods in the literature used to fit the XPS spectra of $Ti_3C_2T_z$. Confusingly, these models make quite different assumptions and each results in different termination chemistries. According to our analysis, none of the existing methods is perfect.

We also make the case that the most physically tenable approach is to fit the Ti $2p_{3/2}$ spectra based on the apexes of the octahedra that surround the Ti atoms. We assign the peak at 455.1 eV C–Ti–O\O\O octahedra. The peaks at 456.0, 457.0, 457.9 eV, are assigned to the C–Ti–O\O\F, C–Ti–O\F\F, C–Ti–F\F\F octahedra, respectively. The peak at 459.6 eV is assigned to $TiO_{2-x}F_{2x}$. The BE of the C atoms sitting in the Ti octahedra in the MX layers is almost always at 282.0 eV. This value appears to be independent of almost all variables, except, possibly, when the Ti_3AlC_2 is etched in molten salts.

The $Ti_3C_2T_z$-affiliated F 1s spectra, like C 1s, were fit with only one peak corresponding to F terminations. Quantifying non-MXene F contributions is much more difficult compared with C 1s and should be avoided if at all possible.

Fitting of the O 1s spectra was the most ambiguous, and a lot more work needs to be carried out to understand the various O terminations. However, we assign the peak at 529.8 eV to C–Ti–O and that at 532.0 eV to C–Ti–OH and/or C–Ti–O/F. Apart from these two, MXene peaks at 530.8 and 533.4 eV were ascribed to $TiO_{2-x}F_{2x}$ and adsorbed H_2O, respectively.

Asymmetric line shapes, similar to those used for fitting spectra of Ti metal, are used in our proposed model. However, given that the behavior of scattered electrons is different in MXenes compared with pure Ti metal, these peak shapes need to be further optimized specifically for MXenes. This is non-trivial as we need to consider interflake and intraflake transport of electrons between MXene sheets and also the role of interlayer species, impurities, etc. Improved synthesis of MXenes flakes coupled with a better understanding of electronic transport in MXenes can help us model better peak shapes specifically for $Ti_3C_2T_z$ MXenes.

Hopefully, future studies can lead to a better understanding leading to more accurate quantification. The help of modelization by DFT calculations is probably required. Finally, this review was focused mainly on $Ti_3C_2T_z$, which is by far the most studied MXene, and even here the XPS fits are not completely understood, so utmost care should be taken while fitting other MXene compositions as findings from $Ti_3C_2T_z$ may or may not directly translate to those fittings.

FITTING METHODS

CasaXPS Version 2.3.19PR1.0 software was used for peak fitting. The XPS spectra were calibrated by setting the valence edge to zero, which was calculated by fitting the valence edge with a step-down function and setting the intersection to 0 eV. Because MXenes are electrically conductive, all MXene-related peaks were fitted using an asymmetric Lorentzian line shape. The oxide peaks, on the other hand, were fitted using a

symmetric Gaussian/Lorentzian line shape. The background was determined using the Tougaard algorithm, which is a built-in function in the CasaXPS software.

To calculate the elemental ratios, the global elemental ratios were first calculated by considering the total areas under the curves and the relative sensitivity factors for each element. This was done with the help of internal tools provided by CasaXPS software. Further, global elemental ratios obtained were multiplied by the percentage of photoemission spectra contribution by the MXene or oxide component. This was calculated for each element individually to obtain the chemical formula shown in Table 11.

ACKNOWLEDGMENTS

This work was funded by the Division of Materials Research of NSF (DMR 1740795). IC2MP acknowledges financial support from the Agence National de la Recherche (reference ANR-18-CE08-014, MXENECAT project), the European Union (ERDF), the Région Nouvelle Aquitaine, and the French research ministry (PhD thesis of M.B.).

We would like to acknowledge and thank Drs. Joseph Halim, Qing Huang, Dmitri Talapin, Johanna Rosen, and Per Persson for sharing the raw data used herein. We would also like to acknowledge Drs. Farley, Biesinger, and Tougaard for their advice on peak fitting and background subtraction.

AUTHOR CONTRIBUTIONS

V.N. and M.W.B. developed the new fitting model and conducted the critical analysis. M.B., C.C., A.H., and S.C. helped with analysis and discussion. All authors helped with writing the manuscript.

DECLARATION OF INTERESTS

The authors declare no competing interests.

REFERENCES

1. Naguib, M., Kurtoglu, M., Presser, V., Lu, J., Niu, J., Heon, M., Hultman, L., Gogotsi, Y., and Barsoum, M.W. (2011). Two-dimensional nanocrystals produced by exfoliation of Ti_3AlC_2. Adv. Mater. *23*, 4248–4253.

2. Verger, L., Xu, C., Natu, V., Cheng, H.-M., Ren, W., and Barsoum, M.W. (2019). Overview of the synthesis of MXenes and other ultrathin 2D transition metal carbides and nitrides. Curr. Opin. Solid State Mater. Sci. *23*, 149–163.

3. Lin, Z., Shao, H., Xu, K., Taberna, P.-L., and Simon, P. (2020). MXenes as high-rate electrodes for energy storage. Trends Chem. *2*, 654–664.

4. Hui, Xiaobin., Ge, Xiaoli., Zhao, Ruizheng., Li, Zhaoqiang., and Yin, Longwei.; Longwei Yin (2020). Interface Chemistry on MXene-Based Materials for Enhanced Energy Storage and Conversion Performance. Advanced Functional Materials, 2005190, https://doi.org/10.1002/adfm.202005190.

5. Montazeri, K., Currie, M., Verger, L., Dianat, P., Barsoum, M.W., and Nabet, B. (2019). Beyond gold: spin-coated Ti_3C_2-based MXene photodetectors. Adv. Mater. *31*, 1903271.

6. Benchakar, M., Natu, V., Elmelegy, T.A., Sokol, M., Snyder, J., Comminges, C., Morais, C., Célérier, S., Habrioux, A., Barsoum, M.W., et al. (2020). On a two-dimensional MoS_2/Mo_2CT_x hydrogen evolution catalyst obtained by the topotactic sulfurization of Mo_2CT_x MXene. J. Electrochem. Soc. *167*, 124507.

7. Carey, M., Hinton, Z., Natu, V., Pai, R., Sokol, M., Alvarez, N.J., Kalra, V., and Barsoum, M.W. (2020). Dispersion and stabilization of alkylated 2D MXene in nonpolar solvents and their pseudocapacitive behavior. Cell Rep. Phys. Sci. *1*, 100042.

8. Shahzad, F., Alhabeb, M., Hatter, C.B., Anasori, B., Man Hong, S., Koo, C.M., and Gogotsi, Y. (2016). Electromagnetic interference shielding with 2D transition metal carbides (MXenes). Science *353*, 1137–1140.

9. Sokol, M., Natu, V., Kota, S., and Barsoum, M.W. (2019). On the chemical diversity of the MAX phases. Trends Chem. *1*, 210.

10. Sun, Z.M. (2011). Progress in research and development on MAX phases: a family of layered ternary compounds. Int. Mater. Rev. *56*, 143–166.

11. Barsoum, M.W. (2013). MAX Phases (Wiley-VCH Verlag GmbH & Co. KGaA).

12. Halim, J., Cook, K.M., Naguib, M., Eklund, P., Gogotsi, Y., Rosen, J., and Barsoum, M.W. (2016). X-ray photoelectron spectroscopy of select multi-layered transition metal carbides (MXenes). Appl. Surf. Sci. *362*, 406–417.

13. Li, M., Lu, J., Luo, K., Li, Y., Chang, K., Chen, K., Zhou, J., Rosen, J., Hultman, L., Eklund, P., et al. (2019). Element replacement approach by reaction with Lewis acidic molten salts to synthesize nanolaminated MAX phases and MXenes. J. Am. Chem. Soc. *141*, 4730–4737.

14. Kamysbayev, V., Filatov, A.S., Hu, H., Rui, X., Lagunas, F., Wang, D., Klie, R.F., and Talapin, D.V. (2020). Covalent surface modifications and superconductivity of two-dimensional metal carbide MXenes. Science *369*, 979–983.

15. Ghidiu, M., Halim, J., Kota, S., Bish, D., Gogotsi, Y., and Barsoum, M.W. (2016). Ion-exchange and cation solvation reactions in Ti3C2 MXene. Chem. Mater. *28*, 3507–3514.

16. Natu, V., Sokol, M., Verger, L., and Barsoum, M.W. (2018). Effect of edge charges on stability and aggregation of $Ti_3C_2T_z$ MXene colloidal

suspensions. J. Phys. Chem. C *122*, 27745–27753.

17. Schultz, T., Frey, N.C., Hantanasirisakul, K., Park, S., May, S.J., Shenoy, V.B., Gogotsi, Y., and Koch, N. (2019). Surface termination dependent work function and electronic properties of $Ti_3C_2T_x$ MXene. Chem. Mater. *31*, 6590–6597.

18. Jiang, X., Kuklin, A.V., Baev, A., Ge, Y., Ågren, H., Zhang, H., and Prasad, P.N. (2020). Two-dimensional MXenes: from morphological to optical, electric, and magnetic properties and applications. Phys. Rep. *848*, 1–58.

19. Lukatskaya, M.R., Bak, S.-M., Yu, X., Yang, X.-Q., Barsoum, M.W., and Gogotsi, Y. (2015). Probing the mechanism of high capacitance in 2D titanium carbide using in situ X-ray absorption spectroscopy. Adv. Energy Mater. *5*, 1500589.

20. Hope, M.A., Forse, A.C., Griffith, K.J., Lukatskaya, M.R., Ghidiu, M., Gogotsi, Y., and Grey, C.P. (2016). NMR reveals the surface functionalisation of Ti_3C_2 MXene. Phys. Chem. Chem. Phys. *18*, 5099–5102.

21. Harris, K.J., Bugnet, M., Naguib, M., Barsoum, M.W., and Goward, G.R. (2015). Direct measurement of surface termination groups and their connectivity in the 2D MXene V_2CT_x using NMR spectroscopy. J. Phys. Chem. C *119*, 13713–13720.

22. Sarycheva, A., and Gogotsi, Y. (2020). Raman spectroscopy analysis of the structure and surface chemistry of $Ti_3C_2T_x$ MXene. Chem. Mater. *32*, 3480–3488.

23. Karlsson, L.H., Birch, J., Halim, J., Barsoum, M.W., and Persson, P.O.Å. (2015). Atomically resolved structural and chemical investigation of single MXene sheets. Nano Lett. *15*, 4955–4960.

24. Magne, D., Mauchamp, V., Célérier, S., Chartier, P., and Cabioc'h, T. (2016). Site-projected electronic structure of two-dimensional Ti_3C_2 MXene: the role of the surface functionalization groups. Phys. Chem. Chem. Phys. *18*, 30946–30953.

25. Hofmann, S. (2013). Auger- and X-Ray Photoelectron Spectroscopy in Materials Science (Springer).

26. Persson, I., Näslund, L.-Å., Halim, J., Barsoum, M.W., Darakchieva, V., Palisaitis, J., Rosen, J., and Persson, P.O.Å. (2017). On the organization and thermal behavior of functional groups on Ti_3C_2 MXene surfaces in vacuum. 2D Mater. *5*, 015002.

27. Benchakar, M., Loupias, L., Garnero, C., Bilyk, T., Morais, C., Canaff, C., et al. (2020). One MAX phase, different MXenes: a guideline to understand the crucial role of etching conditions on $Ti_3C_2T_x$ surface chemistry. Appl. Surf. Sci. *530*, 147209.

28. Guemmaz, M., Mosser, A., and Parlebas, J.-C. (2000). Electronic changes induced by vacancies on spectral and elastic properties of titanium carbides and nitrides. J. Electron. Spectros. Relat. Phenomena *107*, 91–101.

29. Biesinger, M.C., Lau, L.W.M., Gerson, A.R., and Smart, R.S.C. (2010). Resolving surface chemical states in XPS analysis of first row transition metals, oxides and hydroxides: Sc, Ti, V, Cu and Zn. Appl. Surf. Sci. *257*, 887–898.

30. Mousty-Desbuquoit, C., Riga, J., and Verbist, J.J. (1987). Electronic structure of titanium(III) and titanium(IV) halides studied by solid-phase x-ray photoelectron spectroscopy. Inorg. Chem. *26*, 1212–1217.

31. Khazaei, M., Arai, M., Sasaki, T., Chung, C.-Y., Venkataramanan, N.S., Estili, M., Sakka, Y., and Kawazoe, Y. (2013). Novel electronic and magnetic properties of two-dimensional transition metal carbides and nitrides. Adv. Funct. Mater. *23*, 2185–2192.

32. Greczynski, G., and Hultman, L. (2017). C 1s peak of adventitious carbon aligns to the vacuum level: Dire consequences for material's bonding assignment by photoelectron spectroscopy. ChemPhysChem *18*, 1507–1512.

33. Anthony, M.T., and Seah, M.P. (1984). XPS: energy calibration of electron spectrometers. 2—results of an interlaboratory comparison. Surf Interface Anal *6*, 107–115.

34. Halim, J., Lukatskaya, M.R., Cook, K.M., Lu, J., Smith, C.R., Näslund, L.-Å., May, S.J., Hultman, L., et al. (2014). Transparent conductive two-dimensional titanium carbide epitaxial thin films. Chem. Mater. *26*, 2374–2381.

35. Halim, J., Persson, I., Eklund, P., Persson, P.O.Å., and Rosen, J. (2018). Sodium hydroxide and vacuum annealing modifications of the surface terminations of a Ti_3C_2 (MXene) epitaxial thin film. RSC Adv. *8*, 36785–36790.

36. Blyth, R.I., Buqa, H., Netzer, F., Ramsey, M., Besenhard, J., Golob, P., and Winter, M. (2000). XPS studies of graphite electrode materials for lithium ion batteries. Appl. Surf. Sci. *167*, 99–106.

37. Halim, J., Kota, S., Lukatskaya, M.R., Naguib, M., Zhao, M.-Q., Moon, E.J., Pitock, J., Nanda, J., et al. (2016). Synthesis and characterization of 2D molybdenum carbide (MXene). Adv. Funct. Mater. *26*, 3118–3127.

38. Meshkian, R., Lind, H., Halim, J., El Ghazaly, A., Thörnberg, J., Tao, Q., Dahlqvist, M., Palisaitis, J., et al. (2019). Theoretical analysis, synthesis, and characterization of 2D W 1.33 C (MXene) with ordered vacancies. ACS Appl. Nano Mater. *2*, 6209–6219.

39. Halim, J. (2016). An X-Ray Photoelectron Spectroscopy Study of Multilayered Transition Metal Carbides (MXenes) (Dissertation, Drexel University). http://ezproxy2.library.drexel.edu/login?url=https://www.proquest.com/docview/1820918414?accountid=10559.

40. Nyholm, R., Martensson, N., Lebugle, A., and Axelsson, U. (1981). Auger and Coster-Kronig broadening effects in the 2p and 3p photoelectron spectra from the metals 22 Ti- 30 Zn. J. Phys. F Met. Phys. *11*, 1727–1733.

41. Repoux, M. (1992). Comparison of background removal methods for XPS. Surf Interf. Anal *18*, 567–570.

42. Intikhab, S., Natu, V., Li, J., Li, Y., Tao, Q., Rosen, J., Barsoum, M.W., and Snyder, J. (2019). Stoichiometry and surface structure dependence of hydrogen evolution reaction activity and stability of Mo_xC MXenes. J. Catal. *371*, 325–332.

43. Luthin, J., and Linsmeier, C. (2001). Characterization of electron beam evaporated carbon films and compound formation on titanium and silicon. Phys. Scr. *T91*, 134.

44. Kong, F., He, X., Liu, Q., Qi, X., Zheng, Y., Wang, R., and Bai, Y. (2018). Improving the electrochemical properties of MXene Ti_3C_2 multilayer for Li-ion batteries by vacuum calcination. Electrochim. Acta *265*, 140–150.

45. Cao, Y., Deng, Q., Liu, Z., Shen, D., Wang, T., Huang, Q., Du, S., Jiang, N., et al. (2017). Enhanced thermal properties of poly(vinylidene fluoride) composites with ultrathin nanosheets of MXene. RSC Adv. *7*, 20494–20501.

46. Krishnamoorthy, K., Pazhamalai, P., Sahoo, S., and Kim, S.-J. (2017). Titanium carbide sheet based high performance wire type solid state supercapacitors. J. Mater. Chem. A *5*, 5726–5736.

47. Natu, V., Hart, J.L., Sokol, M., Chiang, H., Taheri, M.L., and Barsoum, M.W. (2019). Edge capping of 2D-MXene sheets with polyanionic salts to mitigate oxidation in aqueous colloidal suspensions. Angew. Chem. Int. Ed. *58*, 12655–12660.

48. Wang, X., Garnero, C., Rochard, G., Magne, D., Morisset, S., Hurand, S., Chartier, P., Rousseau, J., et al. (2017). A new etching environment (FeF_3/HCl) for the synthesis of two-dimensional titanium carbide MXenes: a route towards selective reactivity vs. water. J. Mater. Chem. A *5*, 22012–22023.

49. Yoon, Y., Le, T.A., Tiwari, A.P., Kim, I., Barsoum, M.W., and Lee, H. (2018). Low temperature solution synthesis of reduced two dimensional Ti_3C_2 MXenes with paramagnetic behaviour. Nanoscale *10*, 22429–22438.

50. Halim, J., Cook, K.M., Eklund, P., Rosen, J., and Barsoum, M.W. (2019). XPS of cold pressed multilayered and freestanding delaminated 2D thin films of $Mo_2TiC_2T_z$ and $Mo_2Ti_2C_3T_z$ (MXenes). Appl. Surf. Sci. *494*, 1138–1147.

51. Sun, W., Wang, H., Vlcek, L., Peng, J., Brady, A.B., Osti, N.C., Mamontov, E., Tyagi, M., et al. (2020). Multiscale and multimodal characterization of 2D titanium carbonitride MXene. Adv. Mater. Interfaces *7*, 1902207.

52. Gnedenkov, S.V., Opra, D.P., Sinebryukhov, S.L., Kuryavyi, V.G., Ustinov, A.Y., and Sergienko, V.I. (2015). Structural and electrochemical investigation of nanostructured C:TiO_2–$TiOF_2$ composite synthesized in plasma by an original method of pulsed high-voltage discharge. J. Alloys Compd. *621*, 364–370.

53. Wen, C.Z., Hu, Q.H., Guo, Y.N., Gong, X.Q., Qiao, S.Z., and Yang, H.G. (2011). From titanium oxydifluoride ($TiOF_2$) to titania (TiO_2): phase transition and non-metal doping with enhanced photocatalytic hydrogen (H_2) evolution properties. Chem. Commun. (Camb.) *47*, 6138.

54. Sing, M., Glawion, S., Schlachter, M., Scholz, M.R., Goß, K., Heidler, J., Berner, G., and Claessen, R. (2011). Photoemission of a doped Mott insulator: spectral weight transfer and a qualitative Mott-Hubbard description. Phys. Rev. Lett. *106*, 056403.

55. Biesinger, M.C., Payne, B.P., Grosvenor, A.P., Lau, L.W.M., Gerson, A.R., and Smart, R.S.C. (2011). Resolving surface chemical states in XPS analysis of first row transition metals, oxides and hydroxides: Cr, Mn, Fe, Co and Ni. Appl. Surf. Sci. *257*, 2717–2730.

56. McCafferty, E., and Wightman, J.P. (1998). Determination of the concentration of surface hydroxyl groups on metal oxide films by a quantitative XPS method. Surf Interf. Anal *26*, 549–564.

57. Lu, J., Persson, I., Lind, H., Palisaitis, J., Li, M., Li, Y., Chen, K., Zhou, J., et al. (2019). $Ti_{n+1}C_n$ MXenes with fully saturated and thermally stable Cl terminations. Nanoscale Adv. *1*, 3680–3685.

58. Myhra, S., Crossley, J.A.A., and Barsoum, M.W. (2001). Crystal-chemistry of the Ti_3AlC_2 and Ti_4AlN_3 layered carbide/nitride phases—characterization by XPS. J. Phys. Chem. Sol. *62*, 811–817.

59. Natu, V., Pai, R., Sokol, M., Carey, M., Kalra, V., and Barsoum, M.W. (2020). 2D $Ti_3C_2T_z$ MXene synthesized by water-free etching of Ti3AlC2 in polar organic solvents. Chem *6*, 616–630.

60. Seredych, M., Shuck, C.E., Pinto, D., Alhabeb, M., Precetti, E., Deysher, G., Anasori, B., Kurra, N., and Gogotsi, Y. (2019). High-temperature behavior and surface chemistry of carbide MXenes studied by thermal analysis. Chem. Mater. *31*, 3324–3332.

61. Kobayashi, T., Sun, Y., Prenger, K., Jiang, D., Naguib, M., and Pruski, M. (2020). Nature of terminating hydroxyl groups and intercalating water in $Ti_3C_2T_x$ MXenes: a study by 1 H solid-state NMR and DFT calculations. J. Phys. Chem. C *124*, 13649–13655.

62. Wang, H.-W., Naguib, M., Page, K., Wesolowski, D.J., and Gogotsi, Y. (2016). Resolving the structure of $Ti_3C_2T_x$ MXenes through multilevel structural modeling of the atomic pair distribution function. Chem. Mater. *28*, 349–359.

63. Cumpson, P.J. (1999). Angle-resolved XPS depth-profiling strategies. Appl. Surf. Sci. *144–145*, 16–20.

64. Czoska, A.M., Livraghi, S., Chiesa, M., Giamello, E., Agnoli, S., Granozzi, G., Finazzi, E., Valentin, C. Di, and Pacchioni, G. (2008). The nature of defects in fluorine-doped TiO_2. J. Phys. Chem. C *112*, 8951–8956.

65. Mashtalir, O. (2015). Chemistry of Two-Dimensional Transition Metal Carbides (MXenes) (Dissertation, Drexel University). http://ezproxy2.library.drexel.edu/login?url=https://www.proquest.com/dissertations-theses/chemistry-two-dimensional-transition-metal/docview/1712386169/se-2?accountid=10559.

66. Greenlief, C.M., White, J.M., Ko, C.S., and Gorte, R.J. (1985). An XPS investigation of titanium dioxide thin films on polycrystalline platinum. J. Phys. Chem. *89*, 5025–5028.

67. Lu, G., Bernasek, S.L., and Schwartz, J. (2000). Oxidation of a polycrystalline titanium surface by oxygen and water. Surf Sci. *458*, 80–90.

68. Ashton, M., Mathew, K., Hennig, R.G., and Sinnott, S.B. (2016). Predicted surface composition and thermodynamic stability of MXenes in solution. J. Phys. Chem. C *120*, 3550–3556.